Phase transitions in traffic flow on multilane roads

Boris S. Kerner[1,*] and Sergey L. Klenov[2,†]
[1]*GR/PTF, HPC, G021, Daimler AG, 71059 Sindelfingen, Germany*
[2]*Department of Physics, Moscow Institute of Physics and Technology, 141700 Dolgoprudny, Moscow Region, Russia*
(Received 27 May 2009; revised manuscript received 3 August 2009; published 4 November 2009)

Based on empirical and numerical analyses of vehicular traffic, the physics of spatiotemporal phase transitions in traffic flow on multilane roads is revealed. The complex dynamics of moving jams observed in single vehicle data measured by video cameras on American highways is explained by the nucleation-interruption effect in synchronized flow, i.e., the spontaneous nucleation of a narrow moving jam with the subsequent jam dissolution. We find that (i) lane changing, vehicle merging from on-ramps, and vehicle leaving to off-ramps result in different traffic phases—free flow, synchronized flow, and wide moving jams—occurring and coexisting in different road lanes as well as in diverse phase transitions between the traffic phases; (ii) in synchronized flow, the phase transitions are responsible for a non-regular moving jam dynamics that explains measured single vehicle data: moving jams emerge and dissolve randomly at various road locations in different lanes; (iii) the phase transitions result also in diverse expanded general congested patterns occurring at closely located bottlenecks.

DOI: 10.1103/PhysRevE.80.056101 PACS number(s): 89.40.−a, 47.54.−r, 64.60.Cn, 05.65.+b

I. INTRODUCTION. PHASE TRANSITIONS IN VEHICULAR TRAFFIC IN THE FRAMEWORK OF THREE-PHASE TRAFFIC THEORY

Probably, the first theoretical study of an instability of free traffic flow, which should explain traffic breakdown, was made in 1958–1961 by Herman *et al.* [1,2] and Komentani and Sasaki [3]. In this traffic flow model known as the General Motors (GM) model, the instability was explained by a driver reaction time responsible for a time delay in vehicle deceleration leading to driver *overdeceleration* (driver's over-reaction) incorporated later in a huge number of other various traffic flow models (see reviews [4]): if a vehicle begins to decelerate unexpectedly, then the following vehicle starts deceleration with a time delay; as a result, when the time delay is long enough, to avoid collisions, the driver decelerates longer, which leads to a lower speed than the speed of the preceding vehicle. The subsequent deceleration of following vehicles results in the traffic flow instability. In 1994 it was found that this free flow instability is responsible for a first-order phase transition from free flow to wide moving jam(s) ($F \rightarrow J$ transition) [5].

However, in real traffic a spontaneous $F \rightarrow J$ transition is not observed. Instead, traffic breakdown is governed by a first-order phase transition from free flow to synchronized flow ($F \rightarrow S$ transition); in turn, wide moving jams can emerge spontaneously only in the synchronized flow ($S \rightarrow J$ transition). Thus in real traffic wide moving jams emerge spontaneously due to a sequence of $F \rightarrow S \rightarrow J$ transitions [6].

Earlier traffic flow theories and models reviewed in [4] cannot explain $F \rightarrow S \rightarrow J$ transitions (see a criticism of the theories in Refs. [7–10]). For this reason, Kerner introduced three-phase traffic theory (references in [7]) in which there are (i) the free flow, (ii) synchronized flow, and (iii) wide moving jam phases. The synchronized flow and wide moving jam phases associated with congested traffic are defined via the empirical definitions [S] and [J], respectively. A wide moving jam is a moving traffic jam, i.e., a localized structure of great vehicle density and low speed, spatially limited by two jam fronts, which exhibit the characteristic jam feature [J] to propagate through bottlenecks while maintaining the mean velocity of the downstream jam front. Synchronized flow [S] is defined as congested traffic that does not exhibit the jam feature [J]; in particular, the downstream front of synchronized flow is often *fixed* at the bottleneck.

The first three-phase traffic flow models showing the $F \rightarrow S \rightarrow J$ transitions are stochastic microscopic models [11–13]. Later, other three-phase traffic flow models were developed [8,14–19]. Recent simulation results in the framework of three-phase traffic theory can be found in Ref. [20]. $F \rightarrow S$ and $S \rightarrow J$ transitions as well as the resulting synchronized flow and general patterns (SP and GP for short, respectively) (relations between traffic "phases," "patterns," and "states" are explained in Appendix A) occurring under condition that at each location of a multilane road the same traffic phase is realized in different road lanes have been studied in detail [7,8,13].

However, due to vehicle merging from on-ramps and/or lane changing *different traffic phases* can emerge and exist in the *different road lanes at the same road location*. The physics of such phase transitions on multilane roads has not been known and is revealed in this paper [21].

For the understanding of physical results of the paper we should briefly consider the nature of phase transitions in the framework of three-phase traffic theory (Fig. 1) [6,7,22]. The nature of traffic breakdown at a bottleneck is explained by a competition between two opposing tendencies occurring within a random local disturbance in free flow in which the speed is lower and density is greater than in an initial free flow at the bottleneck: (i) a tendency toward synchronized flow due to vehicle deceleration associated with a speed adaptation effect [Fig. 1(a)]; (ii) a tendency toward the initial free flow due to vehicle acceleration associated with an overacceleration effect [Fig. 1(b)].

*boris.kerner@daimler.com
†s-klenov@mtu-net.ru

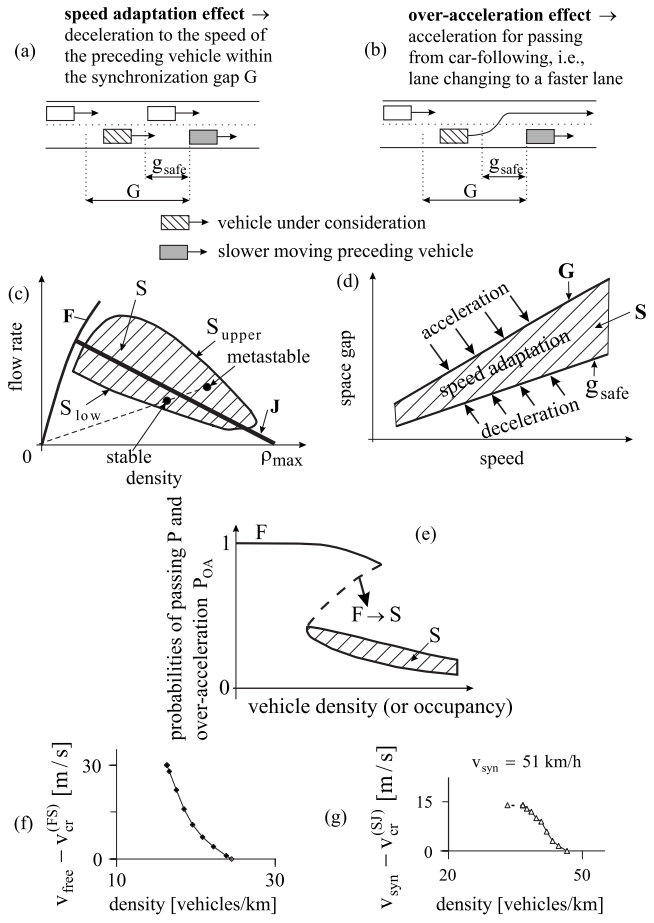

FIG. 1. Explanation of phase transitions in vehicular traffic in the framework of three-phase traffic theory [6,7,22]: [(a) and (b)] Qualitative explanations of speed adaptation (a) and overacceleration (b). (c) Free flow F, a 2D region of steady states of synchronized flow (dashed region), and line J whose slope is determined by the characteristic velocity of the downstream front of a wide moving jam. (d) A part of the 2D region of (c). (e) A qualitative Z-shaped density function for probabilities of passing and overacceleration. [(f) and (g)] Simulation results of Refs. [11,13] for critical speed $v_{cr}^{(FS)}$ required for traffic breakdown in free flow with a speed v_{free} (f) and critical speed $v_{cr}^{(SJ)}$ required for wide moving jam emergence in synchronized flow with a speed v_{syn} (g) as density functions for F→S and S→J transitions, respectively.

The speed adaptation effect is vehicle deceleration occurring under conditions

$$g_{safe} \le g \le G, \tag{1}$$

if a vehicle cannot pass a slower preceding vehicle [Fig. 1(a)]; in Eq. (1), g is a space gap between vehicles, G and g_{safe} are synchronization and safe space gaps, respectively. At $g > G$ the vehicle accelerates, while at $g < g_{safe}$ it decelerates [Fig. 1(d)].

In general, the overacceleration effect is driver maneuver leading to a higher speed from initial car-following at a lower speed occurring under conditions (1). In particular, overacceleration is vehicle acceleration for passing from car-following, i.e., lane changing to a faster lane [Fig. 1(b)]. Then probability of overacceleration denoted by P_{OA} is equal to passing probability P from car-following:

$$P_{OA} = P. \tag{2}$$

In three-phase traffic theory [6,7,22], steady states of synchronized flow cover a two-dimensional (2D) region in the flow-density and space-gap–speed planes [Figs. 1(c) and 1(d)] and at each given density ρ probability of passing P from car-following and, in accordance with Eq. (2), probability for overacceleration is an Z-shaped density characteristic [Fig. 1(e)]. There is a critical probability of overacceleration $P_{OA}^{(cr)}$ [dashed curve between states F and S in Fig. 1(e)] associated with a critical speed $v_{cr}^{(FS)}$ (critical density $\rho_{cr}^{(FS)}$) within a local disturbance required for traffic breakdown [Fig. 1(f)]. When the speed v_{dis} within the disturbance $v_{dis} \le v_{cr}^{(FS)}$ (i.e., the density within the disturbance $\rho_{dis} \ge \rho_{cr}^{(FS)}$), then the disturbance is a nucleus required for traffic breakdown. Within the disturbance the overacceleration effect is on average as strong as or weaker than the speed adaptation effect. This nucleus occurrence causes synchronized flow emergence. Otherwise, when $v_{dis} > v_{cr}^{(FS)}$ ($\rho_{dis} < \rho_{cr}^{(FS)}$), then within the disturbance the overacceleration effect is on average stronger than speed adaptation, therefore no traffic breakdown occurs and free flow remains.

Wide moving jam emergence in synchronized flow (S→J transition) is explained as follows [6,7]: The line J divides the 2D region of steady states of synchronized flow into two different classes [Fig. 1(c)]: (i) states below the line J are stable homogeneous (in space and time) synchronized flow in which no wide moving jams can emerge or persist [labeled "stable" in Fig. 1(c)]. (ii) States on and above the line J are metastable synchronized flow states with respect to wide moving jam emergence [labeled "metastable" in Fig. 1(c)]: if in an initial homogeneous metastable synchronized flow at a given speed v_{syn} a local disturbance with the speed $v_{dis} < v_{syn}$ appears for which $v_{dis} \le v_{cr}^{(SJ)}$, where $v_{cr}^{(SJ)}$ is a critical speed that depends on density [Fig. 1(g)], then the disturbance is a nucleus for an S→J transition called a growing narrow moving jam; the subsequent jam growth leads to wide moving jam emergence.

The paper is organized as follows. In Sec. II, we introduce different physical approaches to the overacceleration effect. These approaches are validated and compared in Sec. III in which spontaneous traffic breakdown outside of bottlenecks is studied. Dual roles of lane changing for phase transitions in free flow and synchronized flow are studied in Secs. IV and V, respectively. An influence of vehicle merging at bottlenecks and lane changing on phase transitions is studied in Sec. VI. Nonregular spatiotemporal traffic dynamics on multilane roads is the subject of Sec. VIII.

II. SIMULATION APPROACHES TO OVERACCELERATION EFFECT

A. Discrete version of stochastic three-phase traffic flow model

For a study of phase transitions on multilane roads in this paper we use a *discrete* (both in time and space) version of our stochastic continuum (in space) three-phase traffic flow

model of Refs. [11,13]. Rather than the continuum space coordinate, a discretized space coordinate with a small enough value of the discretization cell δx is used. Consequently, the vehicle speed and acceleration (deceleration) discretization intervals are $\delta v = \delta x/\tau$ and $\delta a = \delta v/\tau$, respectively.

The physical reason why rather than the continuum model of Refs. [11,13] we introduce and use a new discrete model is as follows. In the continuum model, there are no model fluctuations for the case of a homogeneous in space and time traffic flow [23]. Thus we cannot study spontaneous phase transitions on multilane roads if traffic flow is homogeneous: no lane changing and no fluctuations in this flow would occur in the continuum model. However, to understand the nature of phase transitions on multilane roads, we should first study possible phase transitions due to lane changing in homogeneous traffic flow on multilane roads (see Sec. III below). A formulation of such model fluctuations is easy to perform in a discrete model rather than in the continuum one. This is the main reason for the introducing of the discrete model, which overcomes the above mentioned shortcoming of the continuum model [24].

Update rules of vehicle motion in the discrete model with a new formulation for model speed fluctuations are as follows:

$$v_{n+1} = \max[0, \min(v_{\text{free}}, \tilde{v}_{n+1} + \xi_n, v_n + a\tau, v_{s,n})], \tag{3}$$

$$x_{n+1} = x_n + v_{n+1}\tau, \tag{4}$$

where $n = 0, 1, 2, \ldots$ is number of time steps, τ is a time step, x_n is the vehicle coordinate at time step n, v_n is the vehicle speed at time step n, a is the maximum acceleration, $\tilde{v}_n$ is the vehicle speed without speed fluctuations ξ_n, $v_{s,n}$ is a safe speed at time step n, v_{free} is the maximum speed in free flow, speed fluctuations ξ_n are

$$\xi_n = \begin{cases} \xi_a & \text{if } S_{n+1} = 1 \\ \xi_b & \text{if } S_{n+1} = -1 \\ \xi^{(0)} & \text{if } S_{n+1} = 0, \end{cases} \tag{5}$$

$$\xi_b = a^{(b)}\tau\Theta(p_b - r), \tag{6}$$

$$\xi^{(0)} = a^{(0)}\tau \begin{cases} -1 & \text{if } r < p^{(0)} \\ 1 & \text{if } p^{(0)} \le r < 2p^{(0)} \text{ and } v_n > 0 \\ 0 & \text{otherwise}, \end{cases} \tag{7}$$

S in Eq. (5) denotes the state of vehicle motion ($S_{n+1} = -1$ represents deceleration, $S_{n+1} = 1$ acceleration, and $S_{n+1} = 0$ motion at constant speed), p_b is probability of random deceleration, $p^{(0)}$ and $a^{(0)} \le a$ are constants, $a^{(b)} = a^{(b)}(v_n)$ is a speed function, $r = \text{rand}(0,1)$, $\Theta(z) = 0$ at $z < 0$ and $\Theta(z) = 1$ at $z \ge 0$; the term ξ_a will be explained in Sec. II B.

Because all other functions of the discrete model (3) and their physical meaning are the same as those in the continuum model of [7,13], the complete model and models of bottlenecks as well as model parameters used in simulations below are presented in Tables I–VII of Appendix B.

B. Implicit simulation of overacceleration effect through driver acceleration

The overacceleration effect can be simulated through driver acceleration that occurs under conditions (1) even if the vehicle is not slower than the preceding vehicle and the preceding vehicle does not accelerate. In this approach, the overacceleration effect can be simulated even without lane changing if the function ξ_a in Eq. (5) is taken as [13]

$$\xi_a = a^{(a)}(v_n)\tau\Theta(p_a - r), \tag{8}$$

where p_a is probability of random acceleration, $a^{(a)}(v_n)$ is a vehicle acceleration.

C. Simulation of overacceleration effect through combination of lane changing to faster lane and random driver acceleration

The overacceleration effect can be simulated through the use of a combination of an implicit simulation through a random driver acceleration (8) *and* an explicit simulations based on lane changing to a faster lane: if necessary lane changing rules from the right lane to the left lane $R \to L$ and back $L \to R$ together with some safety conditions presented in Table V of Appendix B are satisfied, the vehicle changes lane with probability p_c [13].

D. "Boundary" overacceleration

In addition with the overacceleration effect *within* a local disturbance of Secs. II B and II C that can be considered a "bulk" overacceleration, there is also a "boundary" overacceleration. The boundary overacceleration effects occurs at the *downstream disturbance front*. We assume that due to boundary overacceleration the mean time delay in vehicle acceleration, which is associated with acceleration probability $p_0(v_n)$ [7],

$$\tau_{\text{del}}^{(a)}(v_n) = \frac{\tau}{p_0(v_n)} \tag{9}$$

can be a decreasing speed function within a speed range between speeds in free and synchronized flows. The reduction in $\tau_{\text{del}}^{(a)}(v_n)$ can be explained by lane changing to a faster lane at the downstream front of the disturbance. To simulate this effect, we use the formula

$$p_0(v) = 0.575 + 0.125 \min(1, v/v_{01}) + 0.15 \max[0, (v - v_{02})/(v_{\text{free}} - v_{02})], \tag{10}$$

where v_{01}, v_{02} are constants, $v_{02} > v_{01}$.

E. Explicit simulation of overacceleration effect through lane changing to faster lane

An explicit simulation of the overacceleration effect through lane changing to a faster lane can be performed through the use of much weaker safety conditions for lane changing in comparison with used in Sec. II C: when these safety conditions are not satisfied, then a vehicle can nevertheless change to a faster lane with the abovementioned given probability p_c, if the space gap between two neighboring vehicles in the target lane satisfies the condition

$$x_n^+ - x_n^- - d > g_{\text{target}}^{(\min)}, \tag{11}$$

where

$$g_{\text{target}}^{(\min)} = \lfloor \lambda v_n^+ + d \rfloor, \tag{12}$$

$\lfloor z \rfloor$ denotes the integer part of a real number z because only integer values of the gap in units of δx are used in the discrete model. In addition, the vehicle should pass the midpoint between two neighboring vehicles in the target lane $x_n^{(m)}$. After lane changing, the coordinate of the vehicle is set to $x_n = x_n^{(m)}$ and the vehicle speed v_n is set to $\hat{v}_n$,

$$\hat{v}_n = \min(v_n^+, v_n + \Delta v^{(1)}). \tag{13}$$

In Eqs. (11)–(13), λ and $\Delta v^{(1)}$ are constants; superscripts + and − in variables, parameters, and functions denote the preceding vehicle and the trailing vehicle in the "target" (neighboring) lane, respectively; the target lane is the lane into which the vehicle wants to change. When this model of overacceleration is used in simulations below, no other mathematical formulations for overacceleration are applied, specifically, $p_a = 0$ in Eq. (8) and rather than Eq. (10), another formula for acceleration probability $p_0(v_n)$ given in Table VII of Appendix B is used.

III. TRAFFIC BREAKDOWN OUTSIDE OF BOTTLENECKS

To study different approaches to modeling of overacceleration effect of Sec. II, we consider traffic breakdown in an initial homogeneous free flow, i.e., on a two-lane road without bottlenecks (Fig. 2). We find that in all modeling approaches to overacceleration of Sec. II, traffic breakdown is a first-order F→S transition, which occurs within a flow rate range

$$q_{\text{th}} \le q \le q_{\max}^{(\text{free})}, \tag{14}$$

where q_{th} is a threshold flow rate for traffic breakdown and $q_{\max}^{(\text{free})}$ is a maximum flow rate [7,11]. In a vicinity of $q_{\max}^{(\text{free})}$, traffic breakdown occurs spontaneously with the subsequent emergence of a moving SP (MSP). However, q_{th} and $q_{\max}^{(\text{free})}$ are very different for the different approaches. In general, we find that the stronger the overacceleration effect, the stronger the tendency to free flow, i.e., the greater $q_{\max}^{(\text{free})}$. On the other hand, the greater $q_{\max}^{(\text{free})}$, the greater the flow rate range [Eq. (14)] in which traffic breakdown can occur.

Thus we find that the greatest overacceleration occurs, when the overacceleration model of Sec. II E is applied [25]. Typical vehicle trajectories during MSP emergence for this model are shown in Fig. 2(c) presented in the coordinate system moving at velocity $v_{\text{system}} = 85$ km/h [Fig. 2(d)]: the speed 85 km/h is close to the maximum synchronized flow speed in the stochastic model. Thus traffic breakdown can be identified through the occurrence of vehicle trajectories with a negative slope associated with the speed $v < 85$ km/h, i.e., with synchronized flow. Due to model fluctuations and lane changing, there are many local disturbances occurring within free flow, however, during about 13.5 min the overacceleration effect overcomes speed adaptation within all these disturbances, therefore, *no* traffic breakdown has occurred. However, lane changing of one of the vehicles [labeled by number 1 in Fig. 2(d)] from the left lane to right lane leads to strong deceleration of following vehicles in the right lane. This results in traffic breakdown in the right lane [labeled by arrow F→S in Fig. 2(d), right]. Later, another vehicle labeled by number 2 in Fig. 2(d) approaching synchronized flow in the right lane changes into the left lane. This leads to a strong deceleration of following vehicles in the left lane. As a result, traffic breakdown occurs also in the left lane leading to MSP formation in both lanes.

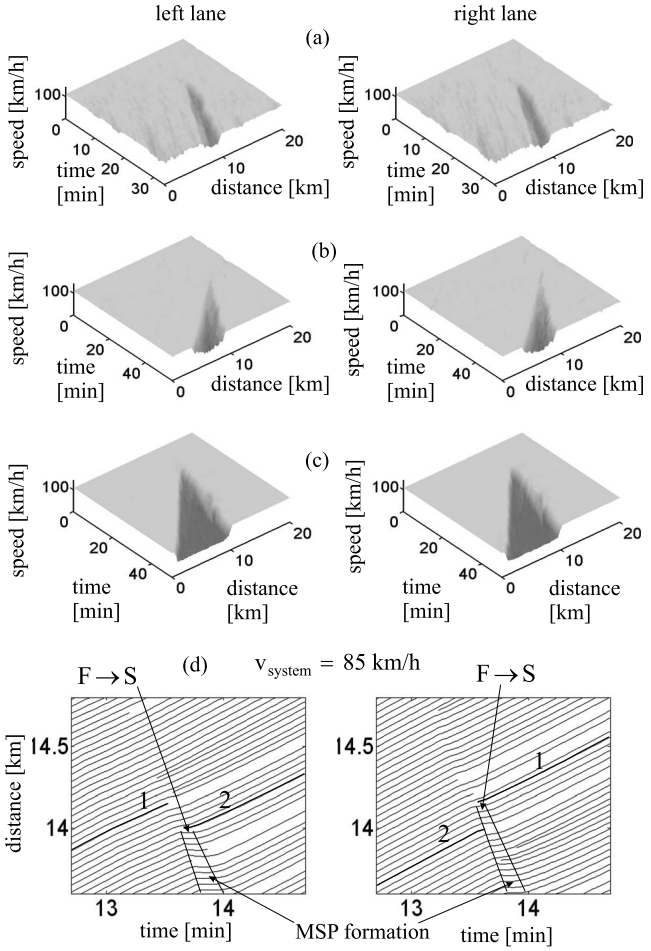

FIG. 2. Simulations of spontaneous traffic breakdown with subsequent MSP emergence on two-lane road without bottlenecks: [(a)–(c)] speed in time and space in the left (figure left) and right lanes (right); models of overacceleration are of Sec. II C for (a), Sec. II D for (b), and Sec. II E for (c) (see model parameters in Table VII); flow rate in initial free flow is 2222 (a), 2345 (b), and 2551 (c) vehicles/h/lane. (d) Vehicle trajectories associated with MSP emergence shown in (c); vehicle trajectories are shown in the coordinate systems moving at the velocity $v_{\text{system}} = 85$ km/h. Resulting values of $q_{\max}^{(\text{free})}$ for different overacceleration models are: 2230 (model of Sec. II C), 2400 (model of Sec. II D), and 2580 vehicles/h/lane (model of Sec. II E).

IV. DUAL ROLE OF LANE CHANGING IN FREE FLOW AT BOTTLENECKS: MAINTENANCE OF FREE FLOW OR TRAFFIC BREAKDOWN

Lane changing can play a dual role in free flow at a bottleneck: lane changing can maintain free flow or in contrast lead to traffic breakdown at the bottleneck:

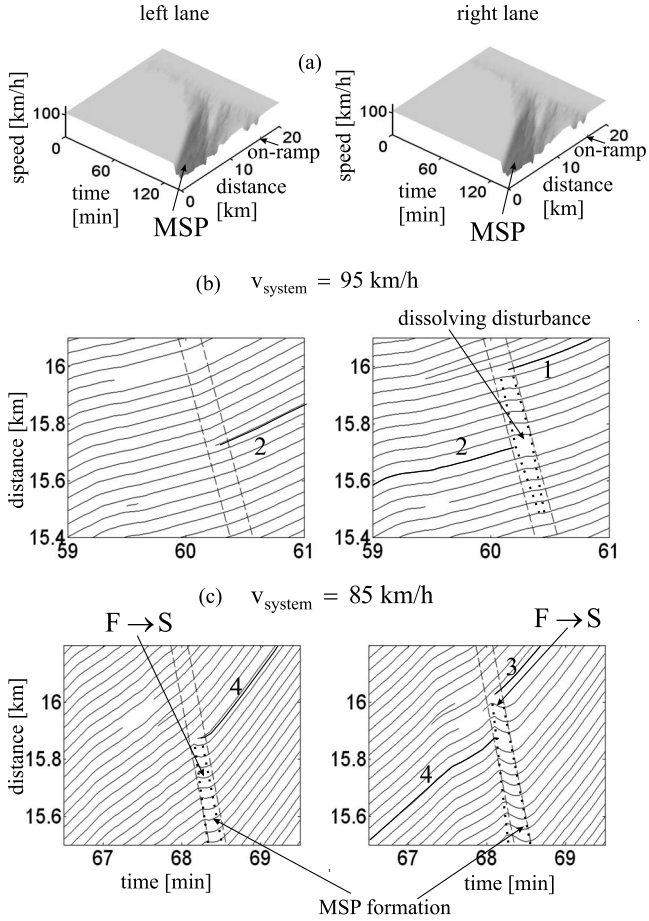

FIG. 3. Simulation of MSP emergence at on-ramp bottleneck: (a) speed in time and space. [(b) and (c)] Vehicle trajectories associated with the MSP emergence at on-ramp bottleneck shown in (a). Vehicle trajectories are shown in the coordinate systems moving at the velocity v_{system}=95 km/h (b) and 85 km/h (c); in these moving coordinate systems, dashed lines show the merging region of the on-ramp of the length 300 m. Figures left and right are related to the left and right road lanes, respectively. Model for overacceleration of Sec. II E. q_{in}=2338 vehicles/h/lane, q_{on}=60 vehicles/h.

(i) Lane changing to a faster lane is responsible for the overacceleration effect that maintains free flow at the bottleneck.

(ii) In contrast, lane changing can lead to the occurrence of a nucleus required for traffic breakdown at a bottleneck. This can occur, if lane changing forces the following vehicles in the target lane to decelerate strongly.

This dual role of lane changing for traffic breakdown at an on-ramp bottleneck is illustrated in Fig. 3. In the coordinate system moving at the velocity v_{system}, the merging region of the on-ramp within which vehicles merge from on-ramp onto the right lane of the main road is moving at a negative velocity $-v_{system}$ [dashed lines in Figs. 3(b) and 3(c)]. The decay of a local disturbance at the bottleneck labeled by "dissolving disturbance" in Fig. 3(b) occurs through lane changing to the faster lane, i.e., through the overacceleration effect. The initial disturbance occurs only in the right lane due to the merging of a vehicle (labeled by number 1) from the on-ramp. However, later one of the vehicles in the right lane [labeled by number 2 in Fig. 3(b)] can pass the slow moving preceding vehicle before the vehicle reaches this disturbance. As a result of this vehicle passing, the initial disturbance in the right lane dissolves over time [dotted curves in Fig. 3(b), right].

The opposite effect of lane changing from the right lane to the left lane leading to an F→S transition in the left lane on the main road is shown in Fig. 3(c), left. First, due to the merging of a vehicle (labeled by number 3) from the on-ramp an initial disturbance occurs only in the right lane. The disturbance grows leading to an F→S transition in the right lane [labeled by arrow F→S in Fig. 3(c), right]: vehicle trajectories with a negative slope within the disturbance associated with synchronized flow ($v<85$ km/h) appear. At the time instant of this traffic breakdown in the right lane, free flow is still observed in the left lane [Fig. 3(c), left)]. Later, one of the vehicles [labeled by number 4 in Fig. 3(c), right] in the right lane can pass the slow moving preceding vehicle. This vehicle passing leads to the deceleration of the following vehicles in the left lane that causes traffic breakdown in the left lane [F→S in Fig. 3(c), left]. As a result, an MSP appears in both lanes.

V. DUAL ROLE OF LANE CHANGING IN SYNCHRONIZED FLOW: MAINTENANCE OF SYNCHRONIZED FLOW OR WIDE MOVING JAM EMERGENCE

Similar opposite effects can occur through vehicle lane changing in synchronized flow: lane changing can either maintain synchronized flow or lead to wide moving jam emergence in synchronized flow. This dual role of lane changing in synchronized flow is as follows: lane changing can lead *either* to the occurrence of a nucleus for the emergence of a wide moving jam in metastable synchronized flow *or* to the dissolution of a moving jam.

A. Empirical study

Empirical examples of these effects are shown in Fig. 4. Empirical vehicle trajectories have been reconstructed from single vehicle data measured through video cameras installed on the road U.S. 101 within a region of about 640 m in a vicinity of on- and off-ramp bottlenecks as shown in Fig. 4(a) [26]. Moving jams emerge and dissolve in synchronized flow that affects both closely located adjacent off- and on-ramp bottlenecks [Fig. 4(a)].

In Fig. 4(b), a moving jam emerges in synchronized flow due to lane changing of vehicles labeled by numbers 1 and 2 from the lane 5 to lane 4. As a result, a moving jam is forming in the lane 4. This effect is similar to empirical moving jam emergence in synchronized flow due to lane changing found in [27].

In contrast, in Fig. 4(c) we show two different examples of the jam dissolution due to lane changing: (i) a moving jam propagating in the lane 5 dissolves after a vehicle labeled by number 3 changes from the lane 5 to lane 6; (ii) a moving jam propagating in the lane 5 dissolves after a vehicle labeled by number 4 changes from the lane 5 to lane 4.

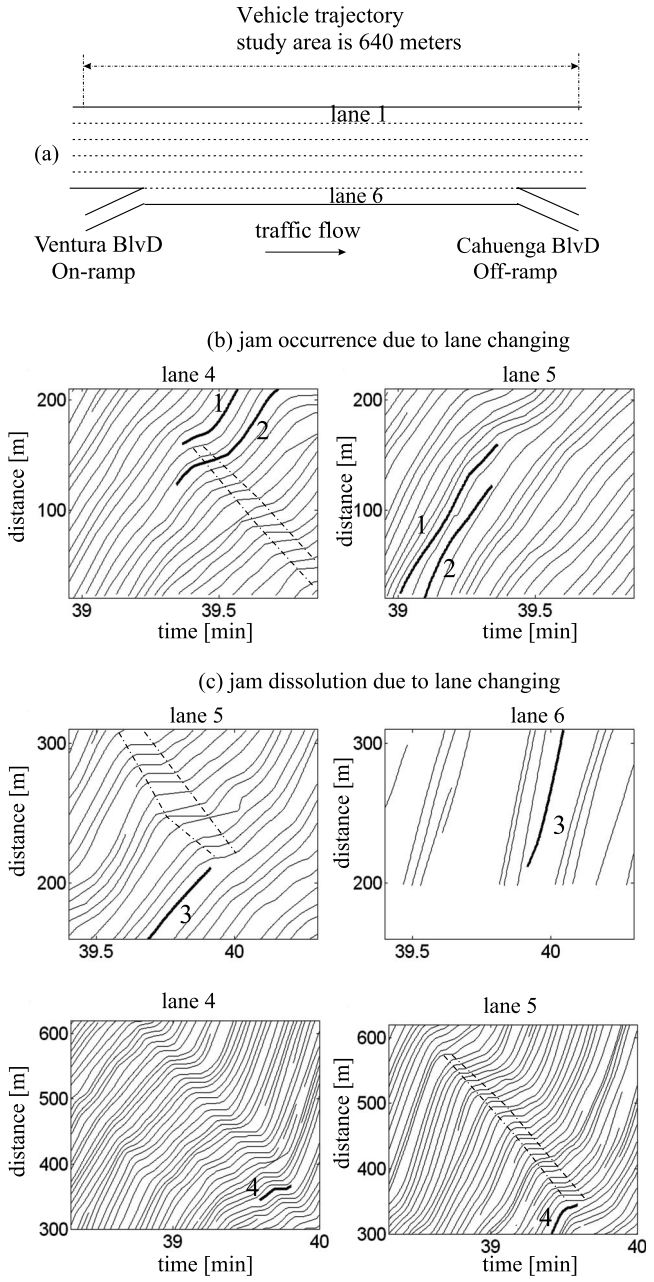

FIG. 4. Empirical study of dual role of lane changing in synchronized flow: (a) Scheme of a section of the road U.S. 101 on which data has been measured. [(b) and (c)] Vehicle trajectories showing the emergence of a wide moving jam (b) and the dissolution of wide moving jams (c) due to lane changing. Moving jams are marked-off by dashed curves. Lanes 1 and 5 are related to the farthest left and right lanes on the main road, respectively; lane 6 is the common merging lane for upstream on- and downstream off-ramp bottlenecks. NGSIM-single vehicle data from June 15, 2005 (without motorcycle data) [26]. In figures time $t=0$ is related to 7:50 a.m. in raw NGSIM-single vehicle data.

B. Numerical simulations

The significance of NGSIM-data (Fig. 4) is that this is *single vehicle* data. In contrast with 1 min average, i.e., *macroscopic* data measured at spatially separated road detectors [7,28], the single vehicle data allow us to study *microscopic* features of moving jam emergence and dissolution in synchronized flow. Because of very expensive measurements of single vehicle data, the data are measured at a very short road section only [Fig. 4(a)]. Therefore, the complete structure of congested patterns associated with the NGSIM-data is *not* known. However, we know from analyses of a huge number of the 1 min average data [7,28] that if many moving jams appear in synchronized flow within a short road section, then due to upstream propagation of congested traffic, an expanded congested pattern (EP) is usually formed whose synchronized flow affects many effectual bottlenecks upstream (Appendix A). Because congested traffic shown in single vehicle data (Fig. 4) should also propagate upstream affecting upstream bottlenecks, we can assume that the NGSIM-data can be associated with a part of an EP cut-out by video cameras installed. This assumption about the EP's part cannot be proven, however, we have proven that there are indeed very many on- and off-ramps on the road U.S. 101 at distances about 0.5 km from each other upstream of the road section under consideration.

For this reason, we simulate an expanded GP (EGP) (Appendix A) occurring on a two-lane road section with *more* than only one on-ramp bottleneck and one off-ramp bottleneck. We discuss here only a part of this EGP labeled by dashed region in Fig. 5(a): as in measured data (Fig. 4), in the simulated EGP's part the distance between the farthest downstream on- and off-ramp bottlenecks is about 500 m. Such simulations increase the application of the physical results for possible future measurements of single vehicle data on longer road sections *and* they do not restrict the applicability of the results for an explanation of NGSIM-data [29]. In addition, an empirical data study made shows that in most cases moving jam emergence and dissolution are associated with lane changing between two neighboring lanes *only*, i.e., possible effects of a cascade of lane changing between three or more lanes are extremely seldom. Thus to study the main physical features of moving jam emergence and dissolution caused by lane changing between two neighboring lanes, we use a two-lane model [30].

To prove that lane changing can lead to the dissolution of moving jams, we consider two of the emergent moving jams in the left lane (labeled by "jam A" and "jam B" in Figs. 5(b) and 6, left). These jams dissolve during their upstream propagation resulting in the maintenance of synchronized flow. Indeed, in Fig. 6(a), a vehicle labeled by number 1 approaching "jam A" changes from the left lane to the right lane. This increases the space gap between vehicles at the upstream jam front; as a result, "jam A" dissolves resulting in synchronized flow (Fig. 6(a), left). A qualitatively similar effect of jam dissolution occurs when a vehicle labeled by number 2 approaching "jam B" in the left lane changes from the left lane to the right lane [Fig. 6(b)].

Two examples of the emergence of moving jams in synchronized flow are shown in Fig. 7. (i) A vehicle labeled by number 3 merges from on-ramp onto the right lane on the main road [Fig. 7(a)]. This vehicle merging causes deceleration of the following vehicles in the right lane. As a result, a growing narrow moving jam occurs in the right lane [jam labeled by "jam C" in Fig. 7(a), right]. (ii) Two vehicles following each other change from the right lane to the left

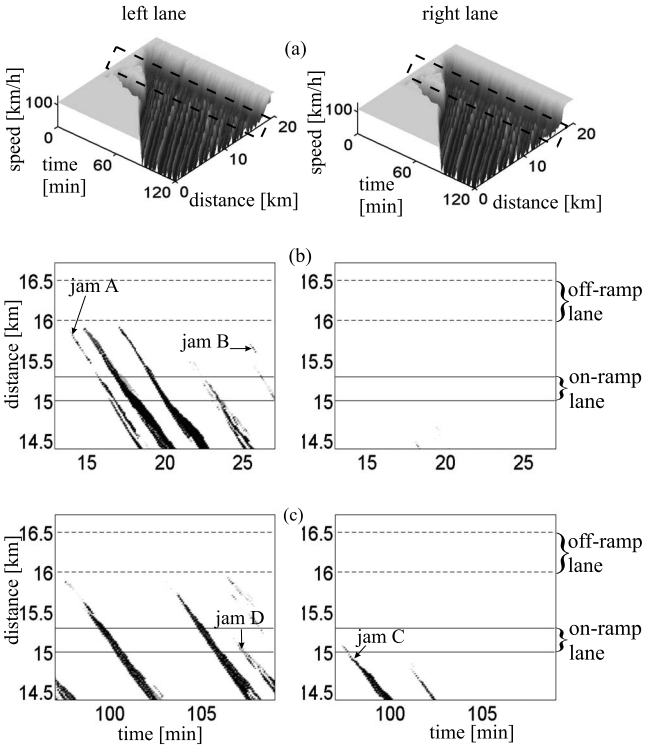

FIG. 5. Simulations of a congested pattern at sequence of five on-ramp and five off-ramp bottlenecks in the left (figures left) and right road lanes (right): (a) 1 min average data for speed in time and space. [(b) and (c)] Single-vehicle speed data for fragments within the pattern in (a) presented by regions with variable darkness (the lower the speed, the darker the region; in white regions the speed is higher than 3 km/h, in black regions the speed is zero). Beginning of merging regions of the on-ramps and off-ramps are at locations $x_{\mathrm{on},i}=7,9,11,13,15$ km and $x_{\mathrm{off},j}=8,10,12,14,16$ km, respectively. Flow rates to on-ramps $q_{\mathrm{on}\ i}$, $i=1,\ldots 5$ and percentage of vehicles leaving the main road to off-ramps η_j, $j=1,\ldots 5$ are: $q_{\mathrm{on}\ i}=500,400,600,720,600$ vehicles/h for $i=1,2,3,4,5$, respectively; $\eta_j=3,15,10,2,70\%$ for $j=1,2,3,4,5$, respectively. $q_{\mathrm{in}}=1500$ vehicles/h/lane. Model for overacceleration of Sec. II E.

lane in which synchronized flow has been before [trajectories 4 and 5 in Fig. 7(b)]. Due to lane changing space gaps between following vehicles in the left lane and, therefore, the vehicle speed decrease considerably. This leads to the emergence of a growing narrow moving jam labeled by "jam D" in Fig. 7(b), left.

VI. INFLUENCE OF VEHICLE MERGING AT BOTTLENECKS AND LANE CHANGING ON PHASE TRANSITIONS

A. Transformation of SP into GP at off- and on-ramp bottlenecks

Merging of vehicles from an on-ramp lane onto the main road or from the left lane to the right lane upstream of an off-ramp can increase the nucleus occurrence for S→J transitions in synchronized flow considerably. This effect on multilane roads is studied in this section with the overacceleration model of Sec. II C.

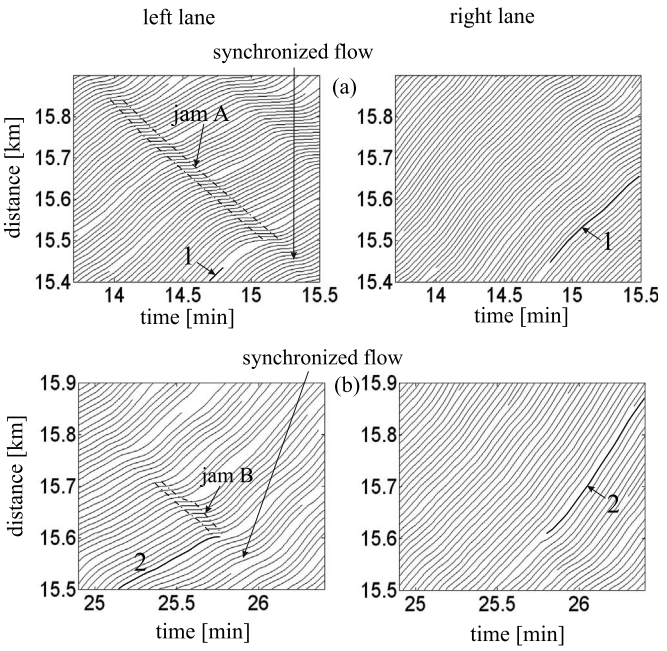

FIG. 6. Simulations of moving jam dissolution resulting in the maintenance of synchronized flow due to lane changing. Vehicle trajectories for two congested pattern fragments shown in Fig. 5(b). Figures left and right are related to the left and right lanes, respectively.

We find that wide moving jams emerge spontaneously more frequently in synchronized flow at a bottleneck, if conditions for vehicles merging become easier; this is simulated through a decrease in the value of λ in Table VI. If λ=0.75,

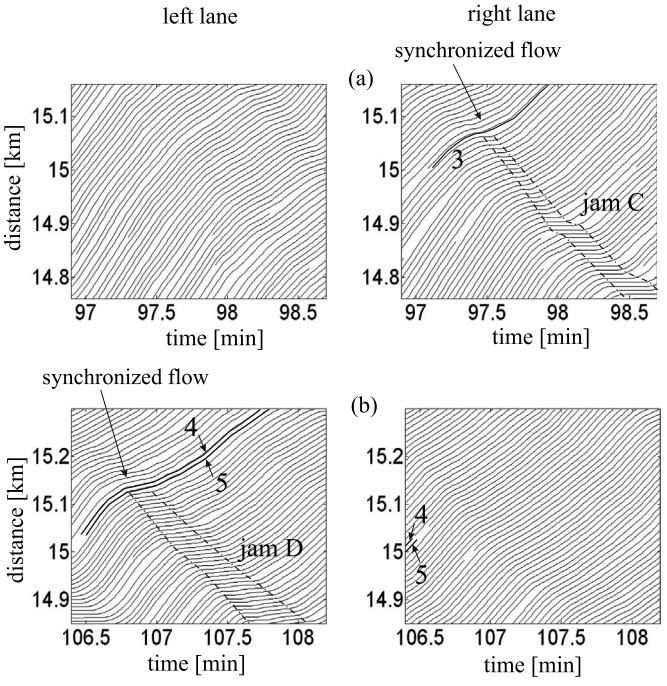

FIG. 7. Simulations of moving jam emergence in synchronized flow due to vehicle merging (a) and lane changing (b). Vehicle trajectories for two congested pattern fragments shown in Fig. 5(c). Figures left and right are related to the left and right lanes, respectively.

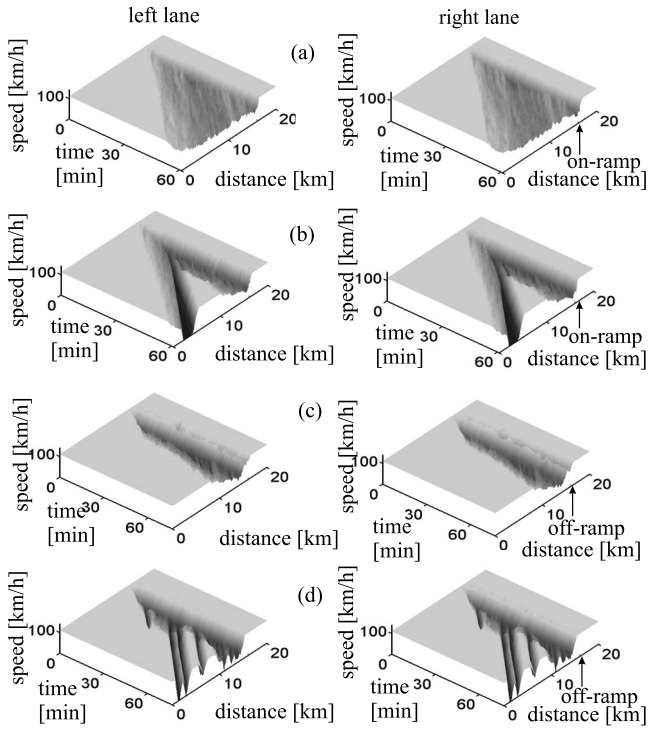

FIG. 8. Transformation of SPs into GPs at on-ramp bottleneck [(a) and (b)] and off-ramp bottleneck [(c) and (d)] at different characteristics for vehicles merging (a)–(d). In (a)–(d), 1 min average speed in space and time in left (left) and right (right) lanes. $q_{\text{in}}=2182$ [(a) and (b)], 1846 vehicles/h/lane [(c) and (d)]. In (a) and (b) $q_{\text{on}}=320$ vehicles/h. In (c) and (d) percentage of vehicles going to the off-ramp $\eta=20\%$.

then a widening SP (WSP) occurs at the on-ramp bottleneck [Fig. 8(a)]. Now if we decrease λ to λ=0.6, then the WSP transforms into an GP [Fig. 8(b)] that is explained as following. Under decrease in λ, some of the vehicles change from the on-ramp lane to the right lane of the main road even if time headways in the right lane are much shorter than a safety time headway. This causes a strong deceleration of the following vehicle. As a result, nuclei for S→J transitions occur with greater probability.

At the off-ramp bottleneck, we find a localized SP (LSP) at λ=0.75 [Fig. 8(c)]. Now, through the decrease in λ to λ=0.6 condition for lane changing from the left lane to the right lane upstream of an off-ramp becomes easier. Then wide moving jams emerge spontaneously within the LSP, i.e., the LSP transforms into an GP [Fig. 8(d)]. The physics of this effect is the same as above for the on-ramp bottleneck.

B. Different phases in different lanes and traffic phase definitions

To study the effect of lane changing on different traffic phases in different lanes [Figs. 9(a)–9(e)], we study a scenario in which in an initial free flow 1 km downstream of an on-ramp bottleneck a wide moving jam is induced in the right lane *only*. We study the effect of this jam in the right lane on congested pattern formation in the left lane for

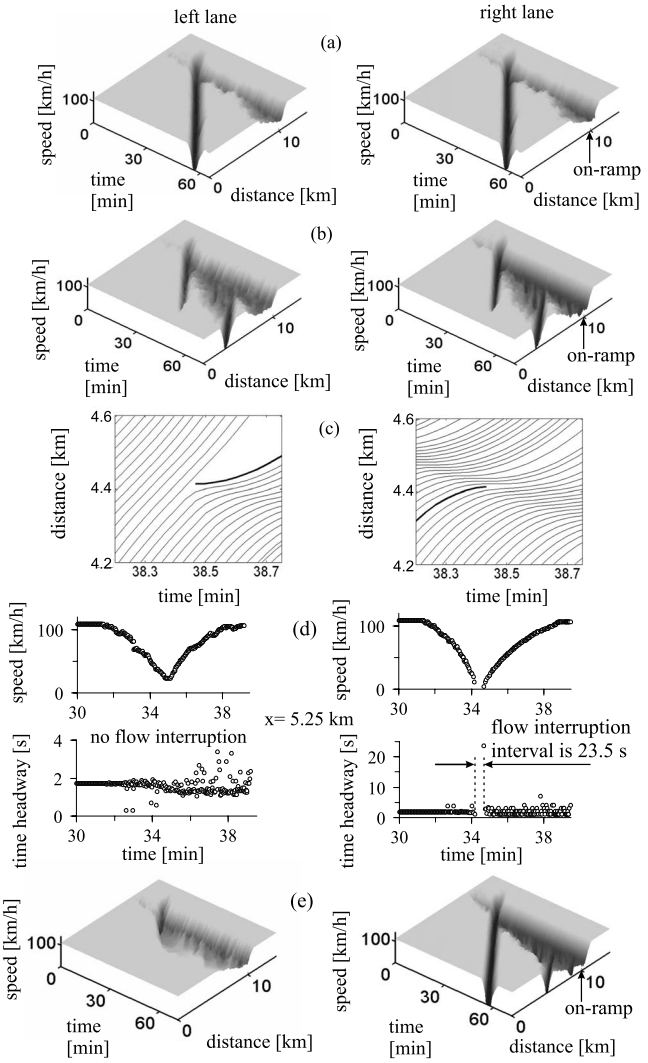

FIG. 9. Simulations of phase transitions between different lanes at different lane changing probabilities p_c: (a) $p_c=0.2$. [(b)–(d)] $p_c=0.02$. (e) $p_c=0.02$ at $x\geq x_{\text{on}}-500$ m and $p_c=0$ at $x<x_{\text{on}}-500$ m. 1 min average speed in time and space in the left (left) and right lanes (right). $x_{\text{on}}=10$ km, $q_{\text{in}}=1846$ vehicles/h/lane, $q_{\text{on}}=540$ vehicles/h. To induce a wide moving jam in the right lane, at $t=t_0=10$ min one of the vehicles in the right lane decelerates to a standstill that lasts 60 s, and then the vehicle accelerates to speed v_{free}. Model for overacceleration of Sec. II C.

different lane changing probabilities p_c: (1) $p_c=0.2$ [Fig. 9(a)], (2) $p_c=0.02$ [Figs. 9(b)–9(d)], (3) $p_c=0.02$ at $x\geq x_{\text{on}}-500$ m and $p_c=0$ at $x<x_{\text{on}}-500$ m [Fig. 9(e)] ($x=x_{\text{on}}$ is the beginning of the on-ramp merging region).

(1) At $p_c=0.2$ lane changing is a relatively frequent one at the jam fronts. As a result, the wide moving jam in the right lane causes a wide moving jam in the left lane [Fig. 9(a)].

(2) At $p_c=0.02$ lane changing is ten times less frequent compared with Fig. 9(a). As a result, we observe the following effects [Figs. 9(b)–9(d)]:

(i) Rather than a wide moving jam, an SP occurs in the left lane [Fig. 9(b)]. Vehicles, which first decelerate within the upstream jam front in the right lane and then change to the left lane, cause deceleration of following vehicles in the left lane [trajectory of such a vehicle is marked by fat black

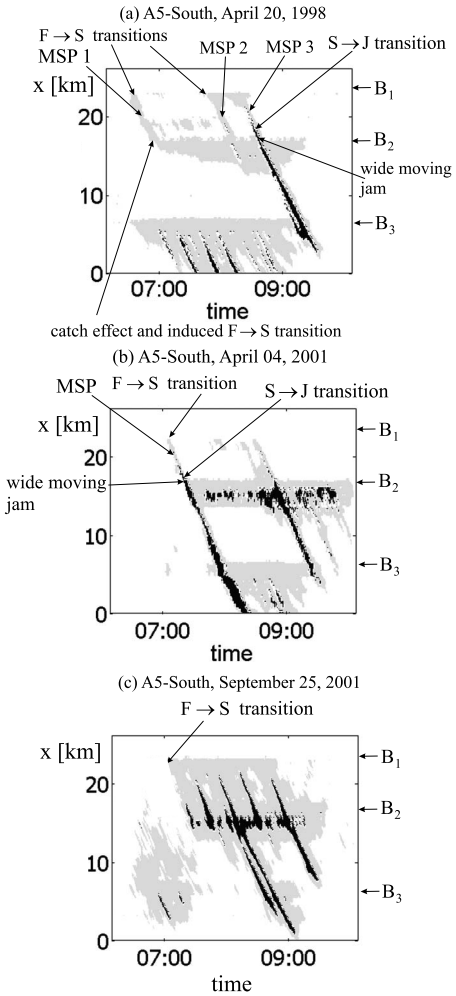

FIG. 10. Emergence of MSPs at off-ramp bottlenecks in macroscopic empirical data: approximate distributions of free flow (white), synchronized flow (gray), and moving jams (black) in space and time. B_1 is off-ramp bottleneck, B_2 and B_3 are on-ramp bottlenecks. Data from the freeway A5-South, Germany. Figure (a) is taken from [7]. Road section sketch is shown in Fig. 2.1 of [7].

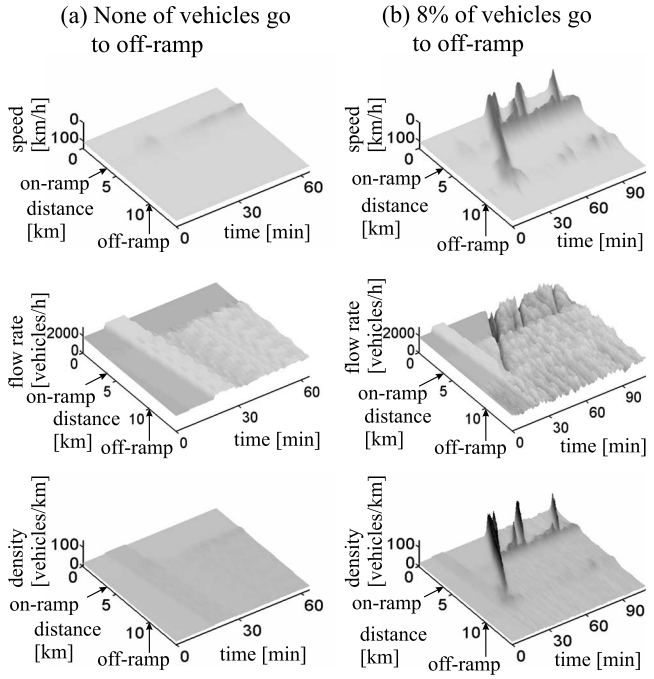

FIG. 11. Speed, flow rate, and density in space and time in the right lane, which are simulated for two different scenarios shown in figures left (a) and right (b) on a two-lane road section with an on-ramp bottleneck located at $x_{on}=3.7$ km and a downstream off-ramp bottleneck located at $x_{off}=10$ km. In both scenarios, there is a local disturbance in free flow propagating downstream; the disturbance is caused by a flow rate increase $\Delta q_{in}=600$ vehicles/h/lane in the flow rate $q_{in}=1800$ vehicles/h/lane upstream of the on-ramp bottleneck applied at $t=t_0=10$ min during a time interval $\Delta t=10$ min. The difference between the two different scenarios is as follows: (a) None of the vehicles go to the off-ramp (figures left). (b) 8% of the vehicles go to the off-ramp (figures right). In (a) and (b), the on-ramp inflow q_{on} is 100 vehicles/h at $t\leq 20$ min, q_{on} increases linear from 100 to 800 vehicles/h during $20<t<40$ min, and q_{on} is 800 vehicles/h at $t\geq 40$ min, $L_c=1$ km, the discrete stochastic model of Sec. II A with overacceleration model of Sec. II E is used.

curve in Fig. 9(c)]. To prove the SP existence, we use the microscopic criterion for a wide moving jam of Ref. [32]:

$$I_s=\frac{\tau_{max}}{\tau_{del}^{(a)}(0)}\gg 1, \tag{15}$$

where τ_{max} is the maximum time headway that characterizes a so-called *flow interruption interval* within a wide moving jam. In the right lane, there is a flow interruption interval $\tau_{max}=23.5$ s [Fig. 9(d)] for which $I_s=13.3$ (in the model $\tau_{del}^{(a)}(0)\approx 1.77$ s). Thus congested traffic in the right lane is a wide moving jam. In contrast, in the left lane *none* of the time headways satisfies Eq. (15), i.e., congested traffic in the left lane is indeed the SP.

(ii) The F→S transition of item (i) in the left lane occurs over the whole time of the jam existence in the right lane. This explains why after the SP in the left lane has reached the bottleneck and led to the breakdown in the left lane at the bottleneck, the SP is observed in the left lane upstream of the bottleneck. However, this SP is *not* associated with "propagation" of the SP through the bottleneck: synchronized flow is subsequently caused by the wide moving jam in the right lane, i.e., by slow vehicles changing from the right lane to the left lane [Figs. 9(b) and 9(c)].

(iii) An additional effect of this lane changing is that the jam inflow in the right lane decreases in comparison with the case of the jams in both road lanes shown in Fig. 9(a). As a result, the jam width decreases slowly over time and finally the jam dissolves [Fig. 9(b)]. This leads also to the dissolution of the SP in the right lane because the SP, as explained in item (ii) above, occurs in the left lane only as long as the wide moving jam persists in the right lane. To prove this, we repeat scenario shown in Fig. 9(b) under an additional condition that vehicles cannot change lane at all locations $x<x_{on}-500$ m upstream of the bottleneck. This condition is related to the existence of two different single-lane roads at $x<x_{on}-500$ m that are merging onto a two-lane road at $x\geq x_{on}-500$ m. Then we can see [Fig. 9(e)] that in accor-

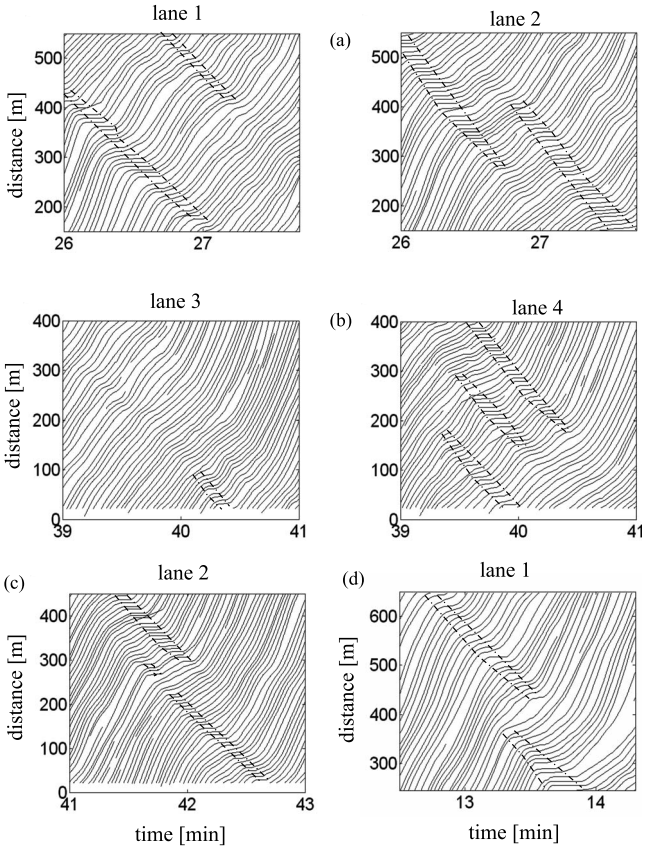

FIG. 12. Empirical vehicle trajectories showing complex nonregular spatiotemporal dynamics of moving jams within synchronized flow that affects the upstream on-ramp and downstream off-ramp bottlenecks on the road U.S. 101 shown in Fig. 4(a). Moving jams are marked-off by dashed curves. NGSIM-single vehicle data measured on June 15, 2005 [26]. In figures time $t=0$ is related to 7:50 a.m. in raw NGSIM-single vehicle data.

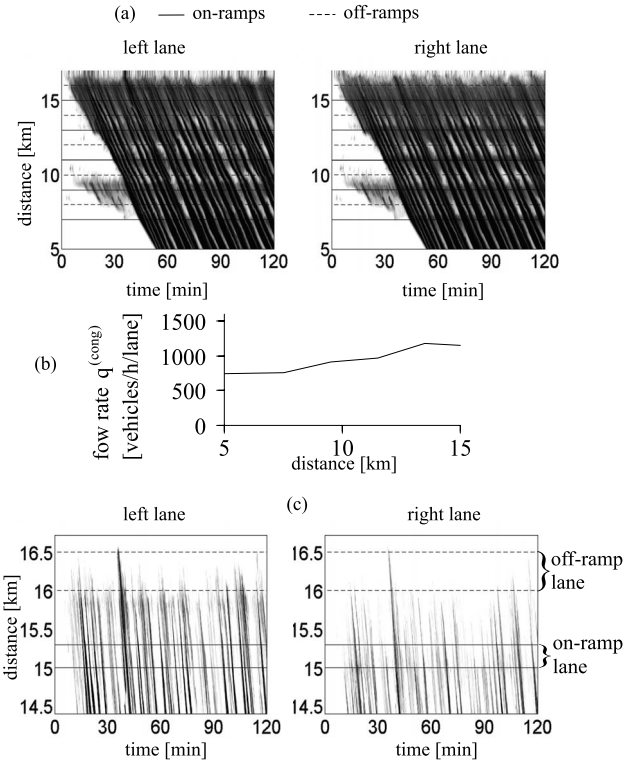

FIG. 13. Analysis of EGP shown in Fig. 5(a): (a) single-vehicle speed data presented in space and time by regions with variable darkness (the lower the speed, the darker the region; in white regions, speeds are higher than 80 km/h; in black regions, speeds are equal to zero). (b) Flow rate $q^{(cong)}$ within the EGP as a function of road location. (c) Jam dynamics in the neighborhood of the farthest on- and off-ramp bottlenecks; in white regions speeds are higher than 20 km/h.

dance with the definition [S] the SP in the left lane caused by the wide moving jam in the right lane is caught at the bottleneck.

C. Emergence of MSPs at off-ramp bottleneck through lane changing upstream of off-ramp

Empirical phase transitions observed in macroscopic traffic data measured on multilane roads can also be often associated with phase transitions caused by lane changing in neighborhoods of on- and off-ramps. In empirical data shown in Fig. 10(a), three different MSPs (labeled by MSP 1, MSP 2, and MSP 3) emerge at an off-ramp bottleneck (labeled by B_1). These MSPs propagate upstream. Two of them (MSP 1 and MSP 2) are caught at an upstream on-ramp bottleneck (labeled by B_2) [31]. However, the MSP 3 transforms into a wide moving jam *before* the MSP 3 reaches the on-ramp bottleneck B_2 (labeled by $S \rightarrow J$ transition): the jam propagates through the on-ramp bottleneck B_2 as well as through the upstream on-ramp bottleneck B_3 while maintaining the mean downstream jam front velocity. Such $F \rightarrow S \rightarrow J$ transitions can also be seen in Fig. 10(b). MSP emergence [Figs. 10(a) and 10(b)] is explained by traffic breakdown at an off-ramp bottleneck due to *lane changing*: Vehicles, which move initially in the passing lane(s) and going to the off-ramp, change to the right lane upstream of the off-ramp (see empirical Fig. 10.8 (b) of [7]) increasing the density in the right lane and fluctuations *upstream* of the off-ramp. This explains why traffic breakdown and the downstream front of resulting congested patterns are observed also upstream of the off-ramp. Whereas the fact that MSPs' emerge at the off-ramp bottleneck B_1 is not clearly seen in Figs. 10(a) and 10(b) without a data analysis in *different lanes* made in [7,28], this fact is clearly seen in Fig. 10(c): the effective location of the off-ramp bottleneck B_1 at which the downstream front of synchronized flow is fixed during a long time interval is exactly *the same one* as that of MSP emergence in Figs. 10(a) and 10(b).

To explain these empirical results, in simulations shown in Fig. 11 we use the same distance between an upstream on- and downstream off-ramp bottlenecks as that in empirical Fig. 10. An initial local disturbance in free flow in which the flow rate and density are greater than outside of the disturbance propagates downstream. If there are *no* vehicles going to the off-ramp, then no traffic breakdown and no moving jam emergence occur [Fig. 11(a)]. However, if at the *same flow rates and disturbance parameters* only 8% of the vehicles go to the off-ramp, then the disturbance causes traffic breakdown with the resulting MSP formation at the off-ramp

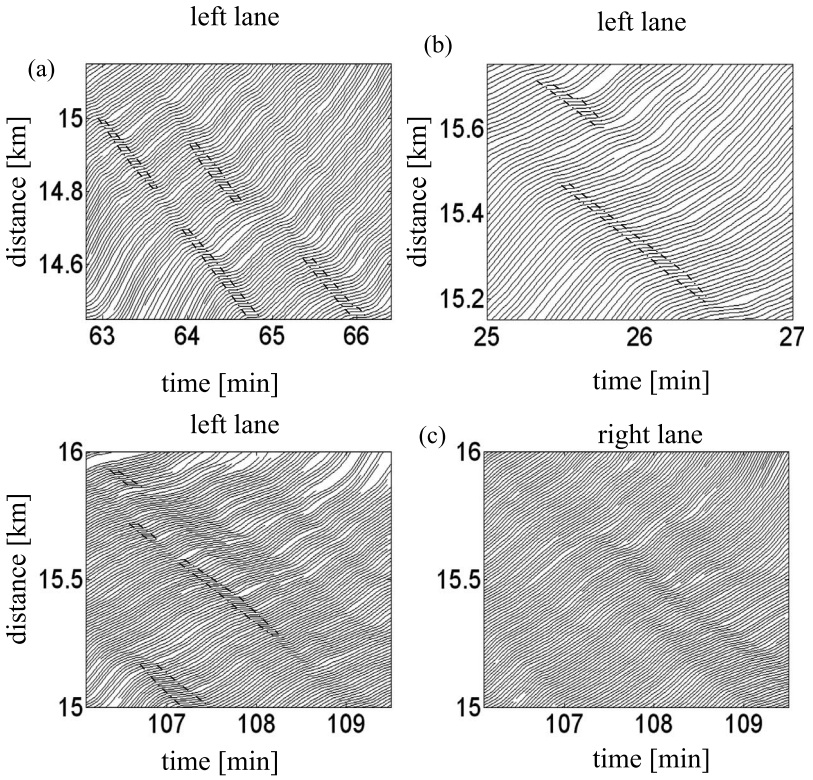

FIG. 14. Simulations of nucleation-interruption effects resulting in complex nonregular spatiotemporal dynamics of narrow moving jams within an EGP in a neighborhood of the farthest on- and off-ramp bottlenecks shown in Fig. 13(c): Vehicle trajectories in space and time in the left lane only [(a) and (b)] and in both lanes (c) for three pattern fragments; moving jams are marked off by dashed curves.

bottleneck [Fig. 11(b)]. As in empirical Fig. 10(b), we find (i) the MSP propagates upstream and transforms into a wide moving jam (at road location about 6.8 km) *before* the MSP reaches the on-ramp bottleneck. (ii) Propagating through the on-ramp bottleneck the jam causes an induced GP formation at the bottleneck [33].

VII. NUCLEATION-INTERRUPTION EFFECTS IN SYNCHRONIZED FLOW

A. Empirical results

If at least two bottlenecks are located very close to each other, as this is the case on the road U.S. 101 [Fig. 4(a)], a complex moving jam dynamics is observed within synchronized flow of an EP (Fig. 12). We can see the following effects of moving jam emergence and dissolution in synchronized flow: moving jams can emerge and dissolve in synchronized flow randomly at different road locations in the different road lanes [Figs. 12(a) and 12(b)] and in a variety of spatiotemporal realizations [Figs. 12(c) and 12(d)].

B. Numerical study

To explain these empirical results, we study EGPs discussed in Sec. V B (Figs. 13–16). We find that in accordance with empirical data (Fig. 12), moving jams can emerge and dissolve in synchronized flow randomly at different road locations in different road lanes and in a variety of spatiotemporal realizations (Figs. 14, 15(c), 15(d), and 16(c)]. This complex jam dynamics is explained by a *nucleation-interruption effect* in synchronized flow of the EGPs: The nucleation-interruption effect is a sequence of the emergence and dissolution of a narrow moving jam in synchronized flow. The effect consists of the following stages: (i) first, a growing narrow moving jam occurs in synchronized flow; (ii) later, this jam dissolves, i.e., the narrow moving jam persists only during a time interval, which is too short for the transformation of the narrow moving jam into a wide moving jam. A variety of the nucleation-interruption effects found in simulations [Figs. 14, 15(c), 15(d), and 16(c)] can explain empirical complex dynamics of narrow moving jams shown in Fig. 12.

The diverse nucleation-interruption effects found in empirical data (Fig. 12) and simulations [Figs. 14, 15(c), 15(d), and 16(c)] can be explained by the following traffic phenomena:

(i) The dual role of lane changing in synchronized flow (Sec. V): lane changing can lead to the occurrence of a nucleus for an $S \rightarrow J$ transition, i.e., to the occurrence of a growing narrow moving jam; in contrast, lane changing can lead to the dissolution of a narrow moving jam, i.e., to the maintenance of synchronized flow. For example, a vehicle labeled by number 1 in Fig. 15(c) changes from the left lane to the right lane; this increases a space gap and leads to the jam dissolution in the left lane. (ii) The increase in the frequency of lane changing in neighborhoods of on- and off-ramp bottlenecks within the EGPs.

In addition to lane changing between lanes on the main road, there are the following effects at the on- and off-ramp bottlenecks that can cause nucleation-interruption effects: (i) vehicle merging from an on-ramp onto the main road can lead to deceleration of the following vehicles resulting in the occurrence of a growing narrow moving jam in synchronized flow on the main road; (ii) vehicles leaving the main road to an off-ramp can lead to the increase in space gaps between

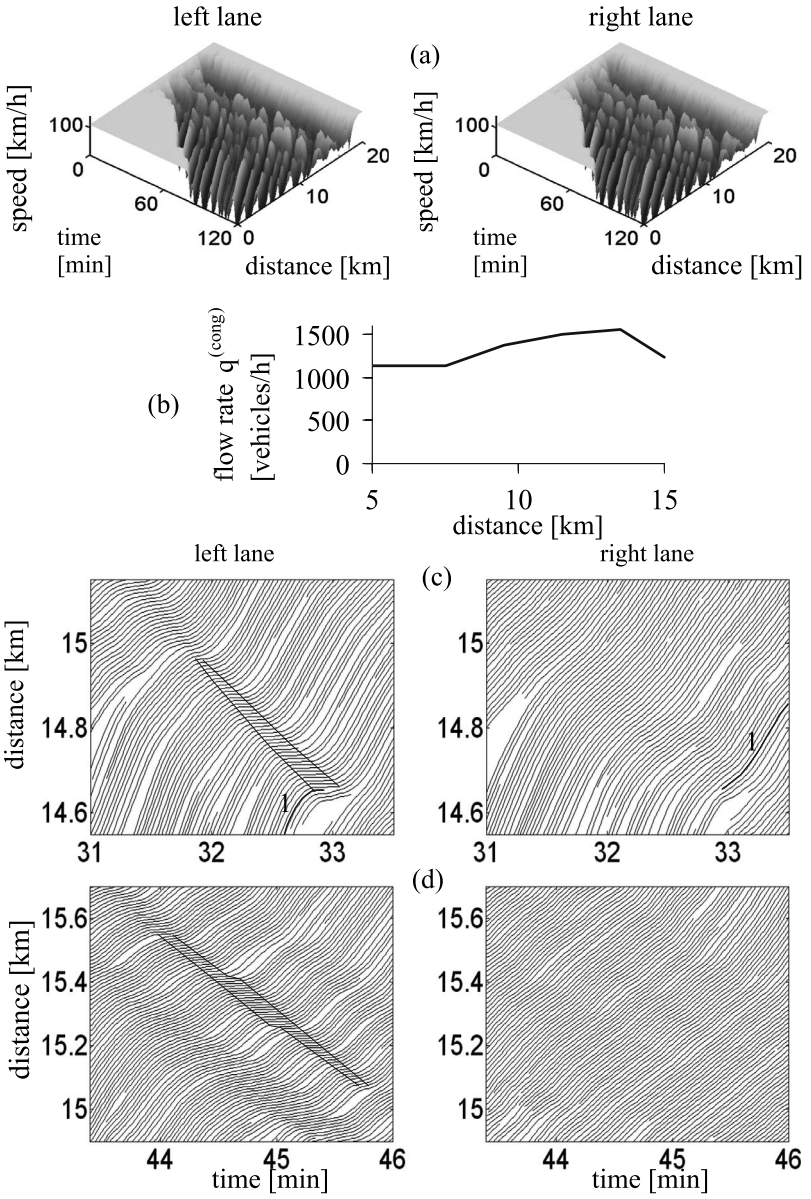

FIG. 15. Simulations of EGP associated with the same adjacent bottlenecks as those in Fig. 5(a), however, at another set of flow rates to on-ramps and percentages of vehicles going to off-ramps: (a) speed in space and time. (b) Flow rate $q^{(cong)}$ within the EGP. [(c) and (d)] Vehicle trajectories within two fragments of the EGP; moving jams are marked off by dashed curves. Flow rates to on-ramps $q_{on\ i}$, $i=1,\ldots,5$ and percentage of vehicles leaving the main road to off-ramps η_j, $j=1,\ldots,5$ are: $q_{on\ i}=500,720,900,900,1200$ vehicles/h for $i=1,2,3,4,5$, respectively; $\eta_j=5,10,20,20,40\%$ for $j=1,2,3,4,5$, respectively.

vehicles moving on the main road resulting in the dissolution of a growing narrow moving jam in synchronized flow on the main road [Fig. 16(c)].

VIII. NONREGULAR SPATIOTEMPORAL DYNAMICS OF WIDE MOVING JAMS ON MULTILANE ROADS

In addition with nucleation-interruption effects of Sec. VII, the complex nonregular dynamics of congested traffic within the EGPs results from spatiotemporal combinations and interactions of the following effects:

(1) The effect of splitting of a flow interruption interval within a wide moving jam into two or more flow interruption intervals [Figs. 17(c), 17(d), and 18(b)]. This splitting effect can result either from the emergence of a new region of moving blanks within the jam or result in the splitting of the jam into two or more wide moving jams [36].

(2) The effect of the emergence of a new flow interruption interval [Figs. 17(a), 17(d), and 18(a)]. This emergence effect can result either from the splitting of a region of moving blanks into two or more regions of moving blanks or result in the emergence of a new wide moving jam (S→J transition).

(3) The effect of the merging of two (or more) flow interruption intervals [Figs. 17(b) and 18(c)]. This merging effect can result either from the dissolution of two (or more) regions of moving blanks within a wide moving jam or result in the merging of two (or more) wide moving jams.

(4) The effect of the dissolution of two (or more) flow interruption intervals [Figs. 17(a), 17(d), and 18(a)]. This dissolution effect can result either from the merging of two (or more) regions of moving blanks within a wide moving jam or result in the dissolution of a wide moving jam.

The same effects have been found in congested traffic occurring at an isolated heavy bottleneck [37], i.e., a bottleneck due to bad weather conditions, accidents or heavy road works causing a very small average flow rate in congested traffic $q^{(cong)} \lesssim 600$ vehicles/h/lane [38]. However, rather than heavy bottleneck conditions congested traffic within the

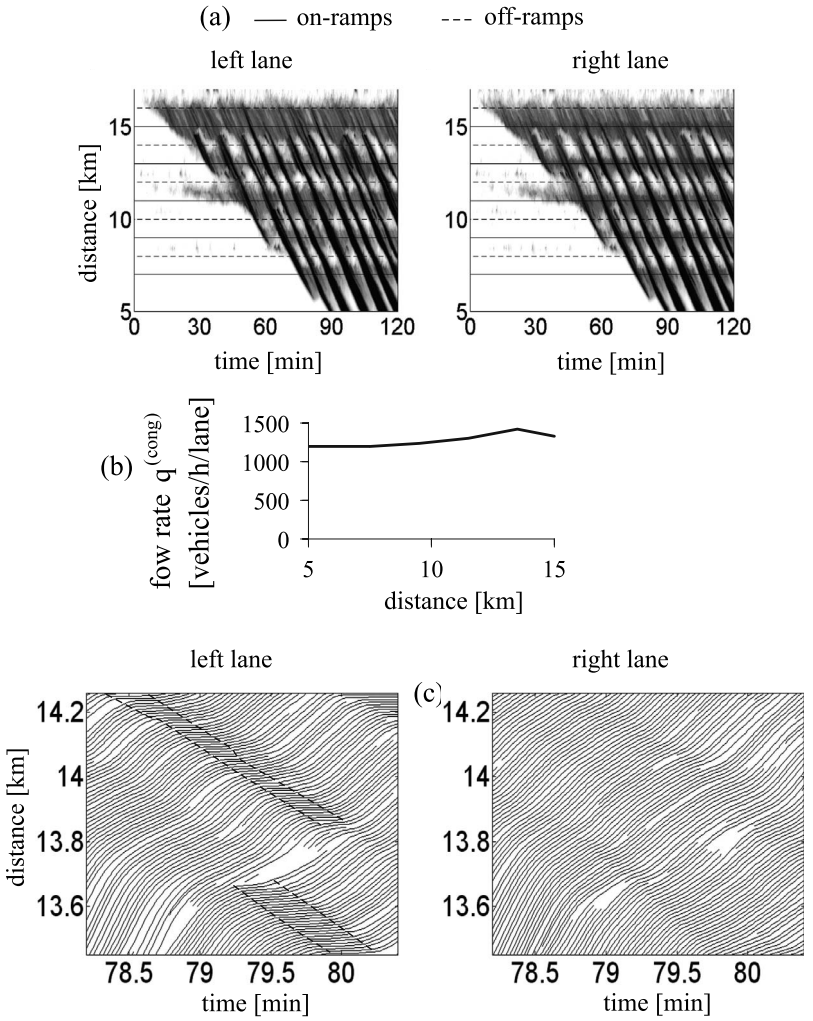

FIG. 16. Simulations of EGP associated with the same adjacent bottlenecks as those in Fig. 5(a), however, at another set of flow rates to on-ramps and percentages of vehicles going to off-ramps: [(a) and (b)] Single-vehicle speed data (a) (in white regions, speeds are higher than 80 km/h; in black regions, speeds are equal to zero) and flow rate $q^{(\mathrm{cong})}$ (b). (c) Vehicle trajectories within a fragment of the EGP; moving jams are marked off by dashed curves. Flow rates to on-ramps $q_{\mathrm{on}\ i}$, $i=1,\ldots,5$ and percentage of vehicles leaving the main road to off-ramps η_j, $j=1,\ldots 5$ are: $q_{\mathrm{on}\ i}=360,450,500,720,600$ vehicles/h for $i=1,2,3,4,5$, respectively; $\eta_j=15,10,20,5,30\%$ for $j=1,2,3,4,5$, respectively.

EGPs shown in Figs. 15 and 16 is associated with usual bottlenecks for which $1100 \lesssim q^{(\mathrm{cong})} \lesssim 1700$ vehicles/h/lane [39]. As a result, we find that in comparison with traffic congestion at a heavy bottleneck [37] in the EPs shown in Figs. 15 and 16 the emergence and dissolution of moving jams occurs very frequently at considerably higher synchronized flow speeds between moving jams. This is explained by a very frequent lane changing to a faster lane used in the model (Sec. II E): the emergence and dissolution of moving jams are mostly caused by the dual role of lane changing in synchronized flow of Sec. V.

Some examples are shown in Figs. 19 and 20: (i) after two vehicles labeled by numbers 1 and 2 in Fig. 19(a) have changed from the right lane to the left lane, blanks between vehicles standing within a flow interruption interval in the right lane appear. Vehicles covering these blanks lead to moving blanks [36] propagating upstream within this flow interruption interval. This results in the splitting of the flow interruption interval into two intervals separated by the region of moving blanks. (ii) After three vehicles labeled by numbers 3–5 in Fig. 19(b) have changed from the right lane to the left lane, new moving blanks in a region of moving blanks in the right lane appear that leads to a widening of the region of moving blanks. However, these vehicles decrease space gaps in a region of moving blanks in the left lane. This can explain the narrowing of the region of moving blanks in the left lane observed over time [Fig. 19(b), left]. Later, this region of moving blanks dissolves in the left lane [Fig. 19(c), left]. As a result, two flow interruption intervals, which have earlier been separated by this region of moving blanks in the left lane, merge into a single flow interruption interval [Fig. 19(c), left].

Rather than only single effects of emergence, splitting, merging, and dissolution of flow interruption intervals, we find often complex sequences of these effects over time (Fig. 20). In Fig. 20(a), three vehicles labeled by numbers 1–3 change from the left lane to the right lane. As a result, space gaps between vehicles increase in the left lane and, therefore, a region of moving blanks emerges in the left lane. First, this region widens over time. However, later vehicles labeled by numbers 4, 5 change from the right lane to the left lane that decrease space gaps between vehicles in the left lane. This leads to the dissolution of the region of moving blanks, i.e., to the merging of the flow interruption intervals. In Fig. 20(b), due to a sequence of lane changing a complex dynamics of the splitting, emergence, and dissolution of flow interruption intervals is observed leading to the nonregular dynamics of wide moving jams.

We find the following results:

(i) The nonregular dynamics of congested traffic within EGPs can be considered resulting from spatiotemporal inter-

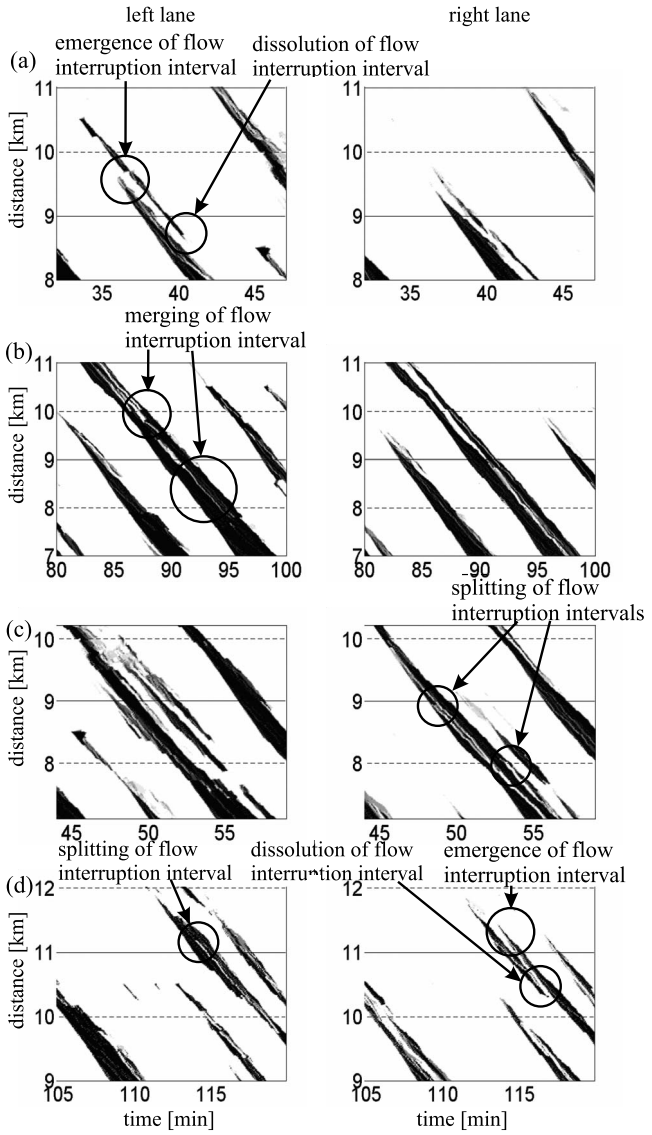

FIG. 17. Fragments of complex nonregular spatiotemporal dynamics of moving jams within the EGP shown in Fig. 15. Single-vehicle speed data presented by regions with variable darkness (the lower the speed, the darker the region; in white regions the speed is higher than 7.2 km/h, in black regions the speed is zero).

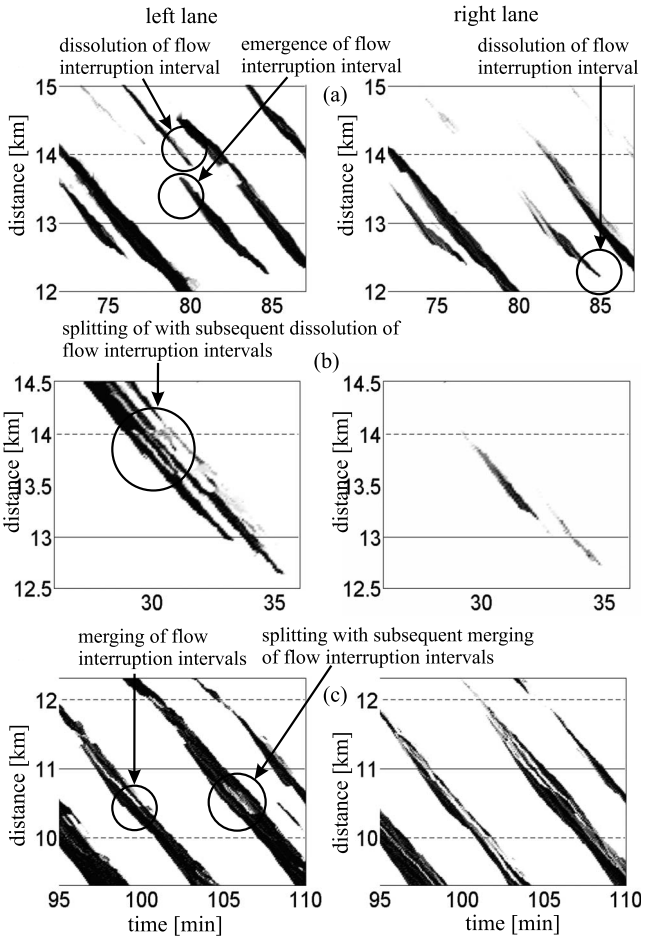

FIG. 18. Fragments of complex non-regular spatiotemporal dynamics of moving jams within the EGP shown in Fig. 16. Single-vehicle speed data presented by regions with variable darkness (the lower the speed, the darker the region; in white regions the speed is higher than 7.2 km/h, in black regions the speed is zero).

actions of the diverse dynamics of synchronized flow and wide moving jams as well as nucleation-interruption effects. In particular, we find that

(1) Lane changing on the main road in synchronized flow leads either to the maintenance of synchronized flow or to the occurrence of nuclei for $S \rightarrow J$ transitions.

(2) Independent of the flow rate $q^{(cong)}$, the nonregular dynamics of moving jams in synchronized flow of the EGPs is associated with the same four effects (splitting, emergence, merging, and dissolution of flow interruption intervals) as those found in congested traffic at an isolated heavy bottleneck [37].

(ii) Peculiarities of the nonregular spatiotemporal dynamics of moving jams within these EGPs are as follows: vehicles going to the off-ramps and vehicles merging from on-ramps cause many nuclei for $S \rightarrow J$ transitions in different lanes within synchronized flow of the EGPs; as a result, a more complicated spatiotemporal dynamics of moving jams occurring at different road locations randomly and independent of each other in the different lanes is observed at the sequence of adjacent bottlenecks than the one found at an isolated bottleneck.

At a given flow rate upstream of the bottlenecks and different sets of on-ramp inflow rates and percentages of vehicles going to different off-ramps we find qualitatively different EGPs: numerical simulations allow us to assume that at the same sequence of adjacent bottlenecks, an *infinite number* of various EGPs with the complex dynamics of congested traffic can be expected at different sets of on-ramp inflow rates and percentage of vehicles going to off-ramps (only four examples are shown in Figs. 13, 15, 16, and 21).

At different sets of the on-ramp inflow rates and percentages of vehicles going to off-ramps we find that (i) either the average flow rate in congested traffic $q^{(cong)}$ satisfies condition for usual bottlenecks (Fig. 16) or $q^{(cong)}$ is very small as that for a heavy bottleneck; (ii) EGPs can occur for which on some road section $q^{(cong)}$ is great as for usual bottlenecks (road locations $13 < x < 15$ km in Fig. 21), whereas on other

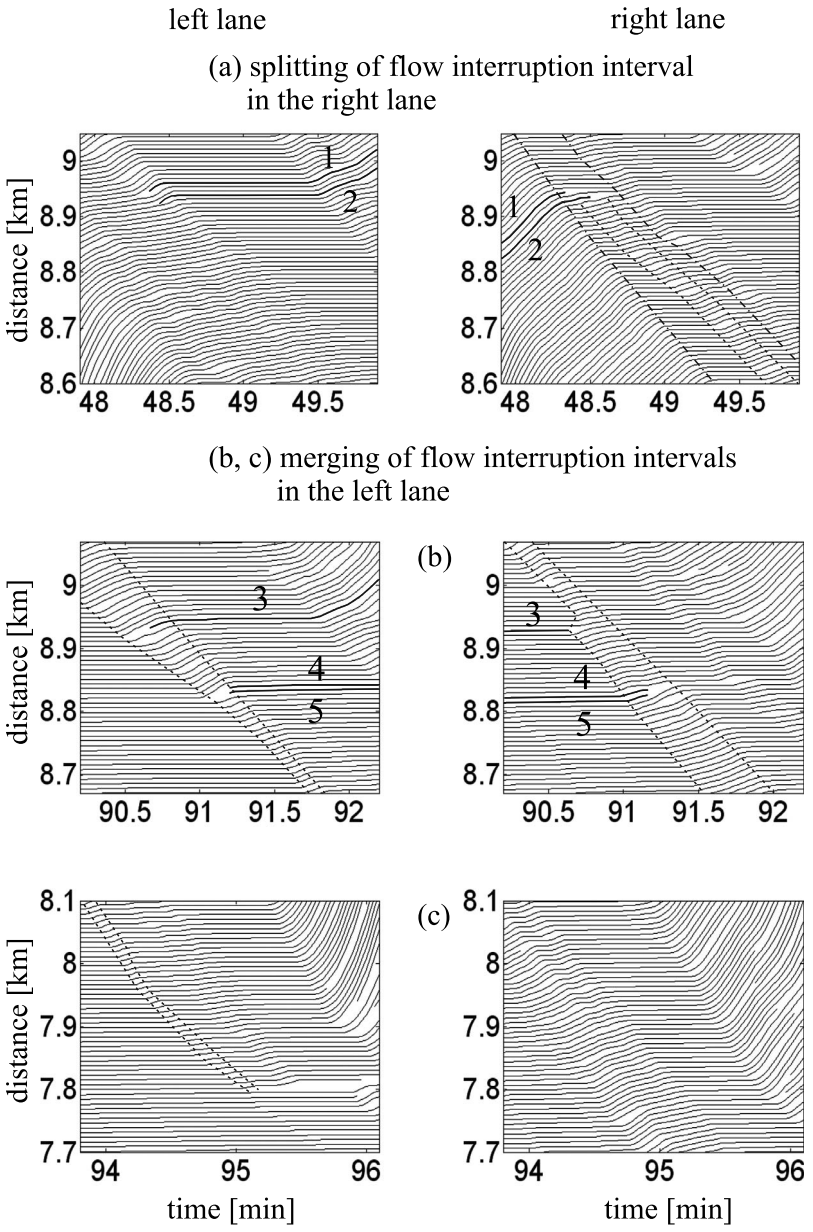

FIG. 19. Vehicle trajectories showing the splitting of flow interruption interval (a) and merging of two flow interruption intervals [(b) and (c)] within EGP fragments shown in Figs. 17(b) and 17(c), respectively.

road locations $q^{(\mathrm{cong})}$ is small, i.e., traffic congestion within the EGPs should be referred to heavy bottleneck conditions (road locations $x<10$ km in Fig. 21).

IX. CONCLUSIONS: PHYSICS OF PHASE TRANSITIONS ON MULTILANE ROADS

(i) The complex dynamics of moving jams observed in empirical single vehicle data measured on highways in the USA is explained by the nucleation-interruption effect in synchronized flow, i.e., the spontaneous nucleation of a narrow moving jam with the subsequent jam dissolution.

(ii) An explicit formulation of the overacceleration effect through vehicle lane changing to a faster lane leads to a *first-order* phase transition from free flow to synchronized flow as observed in real measured data.

(iii) In free flow, lane changing to a faster lane exhibits a dual role: (1) it can lead to the maintenance of free flow (overacceleration effect) or, in contrast, (2) it can cause the occurrence of a nucleus for traffic breakdown in free flow.

(iv) In synchronized flow, lane changing exhibits also a dual role: (1) it can lead to the maintenance of synchronized flow and cause the dissolution of moving jams or, in contrast, (2) it can cause the occurrence of a nucleus, i.e., a growing narrow moving jam whose subsequent growth leads to wide moving jam emergence.

(v) Vehicle merging from on-ramps or vehicle leaving to off-ramps can lead to a frequent occurrence of nuclei for traffic breakdown in free flow or wide moving jam emergence in synchronized flow. However, vehicle leaving to off-ramps can also cause the dissolution of moving jams.

(vi) The nucleation-interruption effect in synchronized flow [item (i)] is caused by a spatiotemporal competition of the nucleation of a narrow moving jam and the jam dissolution, which result often from the dual role of lane changing and vehicle leaving to off-ramps.

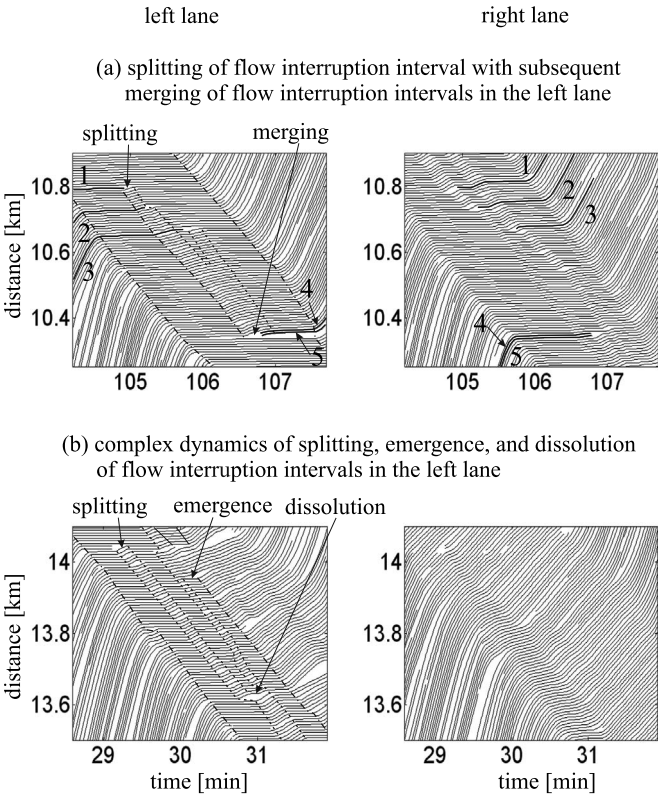

FIG. 20. Vehicle trajectories showing the splitting of flow interruption interval with subsequent merging of the flow interruption interval (a) within EGP fragment shown in Fig. 18(c) and a complex dynamics of splitting, dissolution, and emergence of flow interruption intervals (b) within EGP fragment shown in Fig. 18(b).

(vii) Probability of lane changing exhibits a great effect on the transformation between different congested patterns and their evolution.

(viii) When there are several closely located adjacent highway on- and off-ramp bottlenecks, very complex expanded general patterns (EGP) can occur. A spatiotemporal structure of an EGP, i.e., a combination of the three traffic phases—(1) free flow, (2) synchronized flow, and (3) wide moving jams—in space and time in different road lanes depends qualitatively and quantitatively on a set of the flow rates to on-ramps and percentage of vehicles going to off-ramps. An infinite number of qualitatively different EGPs for different sets of the flow rates to on-ramps and percentage of vehicles going to off-ramps can be expected.

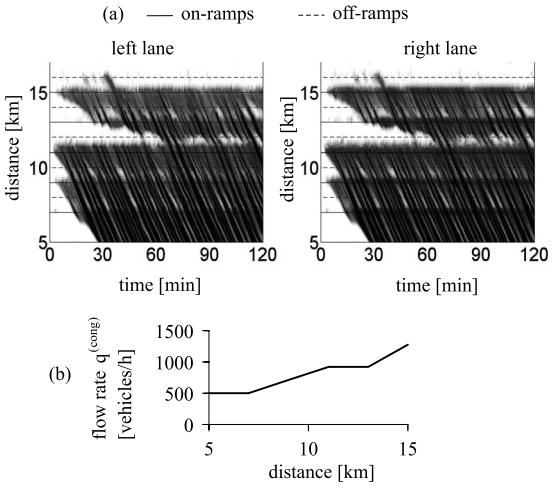

FIG. 21. Simulations of EGP associated with the same adjacent bottlenecks as those in Fig. 5(a), however, at another set of flow rates to on-ramps and percentages of vehicles going to off-ramps: $q_{\text{on } i}=900,900,1200,1200,900$ vehicles/h for $i=1,2,3,4,5$, respectively; $\eta_j=2,5,30,2,10\%$ for $j=1,2,3,4,5$, respectively.

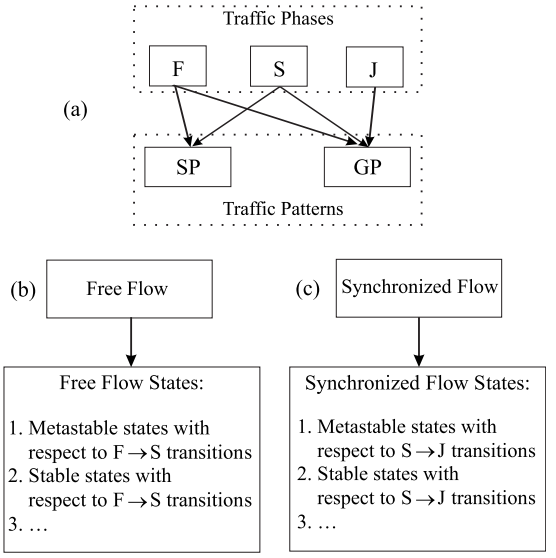

FIG. 22. Explanation of relations between traffic phases, patterns, and states: (a) Relation between traffic phases and main types of congested patterns occurring at a bottleneck; F—free flow, S—synchronized flow, J—wide moving jam. [(b) and (c)] Some examples of different traffic states of the free flow (b) and synchronized flow phases (c).

(ix) Within the EGPs of item (viii), the effects of splitting, emergence, merging, and dissolution of flow interruption intervals within wide moving jams lead to and determine nonregular dynamics of wide moving jams. These effects depend considerably on the frequency of lane changing, vehicle merging from on-ramp and vehicle leaving to off-ramps.

(x) The occurrence and existence of different traffic phases at the same road location in different road lanes, complex phase transitions between them occurring over time, nucleation-interruption effects in synchronized flow, and nonregular dynamics of wide moving jams propagating in

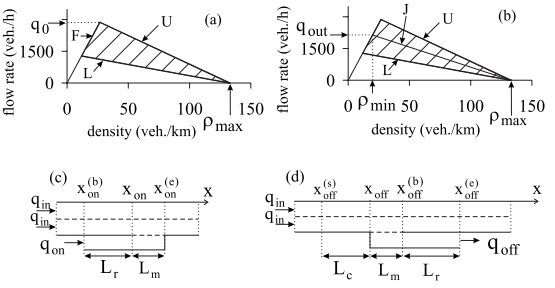

FIG. 23. Steady speed states for the three-phase traffic flow model in the flow-density plane (a) and the line J (b) and models of on-ramp (c) and off-ramp (d) bottlenecks.

TABLE I. Discrete stochastic model.

$$v_{n+1}=\max[0,\min(v_{\text{free}},\tilde{v}_{n+1}+\xi_n,v_n+a\tau,v_{\text{s},n})],$$
$$x_{n+1}=x_n+v_{n+1}\tau,$$
$$\tilde{v}_{n+1}=\max[0,\min(v_{\text{free}},v_{\text{s},n},v_{\text{c},n})],$$
$$v_{\text{c},n}=\begin{cases}v_n+\Delta_n & \text{at } g_n\le G_n,\\ v_n+a_n\tau & \text{at } g_n>G_n,\end{cases}$$
$$\Delta_n=\max[-b_n\tau,\min(a_n\tau,v_{\ell,n}-v_n)],$$
$$g_n=x_{\ell,n}-x_n-d,$$

v_{free}, a, d, and τ are constants; the lower index ℓ marks variables related to the preceding vehicle.

synchronized flow determine the complexity of vehicular traffic on multilane roads.

APPENDIX A: RELATIONS BETWEEN TRAFFIC PHASES, PATTERNS, AND STATES

Relations between traffic phases, patterns, and states are explained in Fig. 22. A spatiotemporal congested traffic pattern (congested pattern for short) is a distribution of traffic flow variables in space and time limited spatially by downstream and upstream pattern fronts; the downstream and upstream fronts separate the pattern from other traffic patterns downstream and upstream, respectively. A front of a traffic pattern is either a moving or motionless region within which one or several of the traffic variables change abruptly in space (and in time, when the front is a moving one).

A traffic pattern can consist of different traffic phases [Fig. 22(a)]. There are two main types of congested patterns occurring at a bottleneck: (i) a synchronized flow pattern (SP) is a congested pattern in which congested traffic consists only of the synchronized flow phase. (ii) A general pattern (GP) is a congested pattern in which congested traffic consists of the synchronized flow and wide moving jam phases.

A congested pattern whose synchronized flow affects at least two adjacent bottlenecks has been called an expanded congested pattern (EP) [7]. Thus an expanded SP (ESP) and an expanded GP (EGP) are an SP and an GP, respectively, whose synchronized flows affect at least two adjacent bottlenecks.

An GP is always a general case of a congested pattern. This is because in three-phase traffic theory there are only the synchronized flow and wide moving jam phases in congested traffic and an GP consists of the both phases. An GP is the generic term for many different types of GPs. Examples of these different GP types are a dissolving GP [7], an GP with a nonregular pinch region [37], and an EGP.

Respectively, an SP is the generic term for many different types of SPs, like a moving SP (MSP), a localized SP (LSP), a widening SP (WSP), and an ESP.

The term a *traffic phase* as a generic term for a multitude of various *traffic states* that exhibit spatiotemporal features of the traffic phase. In other words, there can be different traffic states of the same traffic phase [Figs. 22(b) and 22(c)].

TABLE II. Functions in discrete stochastic model I: stochastic time delay of acceleration and deceleration.

$$a_n=a\begin{cases}1 & \text{if } r_1\le P_0\\ 0 & \text{if } r_1>P_0,\end{cases}\qquad b_n=a\begin{cases}1 & \text{if } r_1\le P_1\\ 0 & \text{if } r_1>P_1,\end{cases}$$
$$P_0=\begin{cases}p_0 & \text{if } S_n\ne 1\\ 1 & \text{if } S_n=1,\end{cases}\qquad P_1=\begin{cases}p_1 & \text{if } S_n\ne -1\\ p_2 & \text{if } S_n=-1,\end{cases}$$
$$S_{n+1}=\begin{cases}-1 & \text{if } \tilde{v}_{n+1}<v_n\\ 1 & \text{if } \tilde{v}_{n+1}>v_n\\ 0 & \text{if } \tilde{v}_{n+1}=v_n,\end{cases}$$

$r_1=\text{rand}(0,1)$, $p_0=p_0(v_n)$, $p_2=p_2(v_n)$ are speed functions, p_1 is constant.

TABLE III. Functions in discrete stochastic model II: Model speed fluctuations.

$$\xi_n=\begin{cases}\xi_{\text{a}} & \text{if } S_{n+1}=1\\ \xi_{\text{b}} & \text{if } S_{n+1}=-1\\ \xi^{(0)} & \text{if } S_{n+1}=0,\end{cases}$$
$$\xi_{\text{a}}=a^{(\text{a})}\tau\begin{cases}1 & \text{if } r\le p_{\text{a}}\\ 0 & \text{if } r>p_{\text{a}},\end{cases}\qquad \xi_{\text{b}}=a^{(\text{b})}\tau\begin{cases}-1 & \text{if } r\le p_{\text{b}}\\ 0 & \text{if } r>p_{\text{b}},\end{cases}$$
$$\xi^{(0)}=a^{(0)}\tau\begin{cases}-1 & \text{if } r\le p^{(0)}\\ 1 & \text{if } p^{(0)}<r\le 2p^{(0)} \text{ and } v_n>0\\ 0 & \text{otherwise},\end{cases}$$

$r=\text{rand}(0,1)$, p_{a}, p_{b}, $p^{(0)}$, $a^{(0)}$ are constants. $a^{(\text{a})}=a^{(\text{a})}(v_n)$ and $a^{(\text{b})}=a^{(\text{b})}(v_n)$ are speed functions.

APPENDIX B: DISCRETE STOCHASTIC THREE-PHASE TRAFFIC FLOW MODEL AND MODEL PARAMETERS

A discrete in space and time stochastic model follows from the stochastic continuum in space three-phase traffic

TABLE IV. Functions in discrete stochastic model III: synchronization gap G_n and safe speed $v_{\text{s},n}$.

$$G_n=G(v_n,v_{\ell,n}),$$
$$G(u,w)=\max(0,\lfloor k\tau u+a^{-1}u(u-w)\rfloor),$$

$k>1$ is constant.

$$v_{\text{s},n}=\min(v_n^{(\text{safe})},g_n/\tau+v_\ell^{(\text{a})}),$$
$$v_\ell^{(\text{a})}=\max[0,\min(v_{\ell,n}^{(\text{safe})},v_{\ell,n},g_{\ell,n}/\tau)-a\tau],$$

$v_n^{(\text{safe})}=v^{(\text{safe})}(g_n,v_{\ell,n})$ is taken as that in [40], which is a solution of the Gipps's equation [41].

$v^{(\text{safe})}\tau_{\text{safe}}+X_{\text{d}}(v^{(\text{safe})})=g_n+X_{\text{d}}(v_{\ell,n})$, where τ_{safe} is a safe time gap,

$$X_{\text{d}}(u)=b\tau^2\left(\alpha\beta+\frac{\alpha(\alpha-1)}{2}\right),$$

$\alpha=\lfloor u/b\tau\rfloor$ and $\beta=u/b\tau-\alpha$ are the integer and fractional parts of $u/b\tau$, respectively; b is constant.

TABLE V. Lane changing rules from the right lane to the left lane ($R \to L$) and from the left lane to the right lane ($L \to R$) and safety conditions for lane changing [13].

$R \to L: v_n^+ \geq v_{\ell,n} + \delta_1$ and $v_n \geq v_{\ell,n}$,
$L \to R: v_n^+ > v_{\ell,n} + \delta_1$ or $v_n^+ > v_n + \delta_1$.
Safety conditions:
$g_n^+ > \min(v_n \tau, G_n^+)$,
$g_n^- > \min(v_n^- \tau, G_n^-)$,
$G_n^+ = G(v_n, v_n^+)$, $G_n^- = G(v_n^-, v_n)$,
$G(u,w)$ is given in Table IV.

flow model of Refs. [11,13], if rather than the continuum space coordinate a discretized space coordinate with a small enough value of the discretization cell δx is used. As for the continuum model, for the discrete model hypothetical steady states of synchronized flow cover a two-dimensional (2D) region in the flow-density plane [Figs. 23(a) and 23(b)]. However, because the speed v and space gap g are integer in the discrete model, the steady states do not form a continuum in the flow-density plane as they do in the continuum model. The inequalities

$$g \leq G \quad \text{and} \quad \mathrm{v} \leq \min[\mathrm{v}_{\mathrm{free}}, \mathrm{v}_{\mathrm{s}}(\mathrm{g}, \mathrm{v})] \tag{B1}$$

define a 2D region in the flow-density plane in which the steady states exist for the discrete model. Update rules of vehicle motion in the resulting discrete model are presented in Tables I–V. Open road boundary conditions are applied. Models of vehicle merging at highway bottlenecks [Fig. 23(c) and 23(d)] taken from [7,13] are presented in Table VI; we should note that safety conditions for lane changing of Sec. II E are the same as those used for vehicle merging in the bottleneck models. Model parameters are given in Table VII; remaining model parameters are given in figure captions.

TABLE VI. Models of vehicle merging at bottlenecks that occurs when a safety rule (*) *or* a safety rule (**) is satisfied [13].

Safety rule (*):
$g_n^+ > \min[\hat{v}_n \tau, G(\hat{v}_n, v_n^+)]$,
$g_n^- > \min[v_n^- \tau, G(v_n^-, \hat{v}_n)]$,
$\hat{v}_n = \min(v_n^+, v_n + \Delta v_r^{(1)})$,
$\Delta v_r^{(1)} > 0$ is constant.
Safety rule (**):
$x_n^+ - x_n^- - d > \lfloor \lambda v_n^+ + d \rfloor$,
$x_{n-1} < x_{n-1}^{(\mathrm{m})}$ and $x_n \geq x_n^{(\mathrm{m})}$
or $x_{n-1} \geq x_{n-1}^{(\mathrm{m})}$ and $x_n < x_n^{(\mathrm{m})}$,
$x_n^{(\mathrm{m})} = \lfloor (x_n^+ + x_n^-)/2 \rfloor$,
λ is constant.
Parameters after vehicle merging:
$v_n = \hat{v}_n$,
under the rule (*): x_n maintains the same,
under the rule (**): $x_n = x_n^{(\mathrm{m})}$.
Speed adaptation before vehicle merging

$$v_{\mathrm{c},n} = \begin{cases} v_n + \Delta_n^+ & \text{at } g_n^+ \leq G(v_n, \hat{v}_n^+), \\ v_n + a_n \tau & \text{at } g_n^+ > G(v_n, \hat{v}_n^+), \end{cases}$$

$\Delta_n^+ = \max[-b_n \tau, \min(a_n \tau, \hat{v}_n^+ - v_n)]$,
$\hat{v}_n^+ = \max[0, \min(v_{\mathrm{free}}, v_n^+ + \Delta v_r^{(2)})]$,
$\Delta v_r^{(2)}$ is constant.

TABLE VII. Model parameters used in most simulations (when other model parameters are used, they are given in figure captions).

Parameters for vehicle motion in road lane:
$\tau = \tau_{\mathrm{safe}} = 1$ s, $d = 7.5$ m/δx, $\delta x = 0.01$ m,
$v_{\mathrm{free}} = 30$ ms^{-1}/δv, $b = 1$ ms^{-2}/δa, $\delta v = 0.01$ ms^{-1},
$\delta a = 0.01$ ms^{-2}, $k = 3$, $p_1 = 0.3$, $p_b = 0.1$,
$p^{(0)} = 0.005$, $p_2(v_n) = 0.48 + 0.32\Theta(v_n - v_{21})$,
$v_{01} = 10$ ms^{-1}/δv, $v_{21} = 15$ ms^{-1}/δv, $a = 0.5$ ms^{-2}/δa.
Models for overacceleration of Secs. II B and II C:
$p_0(v_n) = 0.575 + 0.125 \min(1, v_n/v_{01})$,
$a^{(0)} = a^{(\mathrm{a})} = a^{(\mathrm{b})} = a$, $p_a = 0.17$.
Model for overacceleration of Sec. II D:
$p_0(v_n) = 0.575 + 0.125 \min(1, v_n/v_{01}) +$
$+0.15 \max(0, (v_n - v_{02})/(v_{\mathrm{free}} - v_{02}))$,
$v_{02} = 23.61$ ms^{-1}/δv,
$a^{(0)} = a^{(\mathrm{a})} = a^{(\mathrm{b})} = a$. $p_a = 0.17$.
Model for overacceleration of Sec. II E:
$p_0(v_n) = 0.575 + 0.125 \min(1, v_n/v_{01})$,
$a^{(\mathrm{b})}(v_n) = 0.2a +$
$+0.8a \max(0, \min(1, (v_{22} - v_n)/\Delta v_{22}))$,
$a^{(0)} = 0.2a$, $p_a = 0$, $v_{22} = 12.5$ ms^{-1}/δv,
$\Delta v_{22} = 2.778$ ms^{-1}/δv.
Lane changing parameters:
$\delta_1 = 1$ ms^{-1}/δv, $L_a = 150$ m/δx,
$p_c = 0.2$, $\lambda = 0.75$, $\Delta v^{(1)} = 2$ ms^{-1}/δv.
Parameters of bottleneck models:
$\lambda = 0.75$ or 0.6 for on- or off-ramps,
$v_{\mathrm{free\ on}} = 22.2$ ms^{-1}/δv, $v_{\mathrm{free\ off}} = 25$ ms^{-1}/δv,
$\Delta v_{\mathrm{r}}^{(2)} = 5$ or -2.5 ms^{-1}/δv for on- or off-ramps,
$L_{\mathrm{r}} = 1$ km/δx, $L_{\mathrm{c}} = 0.7$ km/δx, $\Delta v_{\mathrm{r}}^{(1)} = 10$ ms^{-1}/δv,
$L_{\mathrm{m}} = 0.3$ or 0.5 km/δx for on- or off-ramps.

Note that model fluctuations in homogeneous free flow introduced in the model of overacceleration of Sec. II E are chosen smaller than that in synchronized flow that is explained as follows: traffic breakdown is explained by a competition of speed adaptation and overacceleration that exhibits a discontinuous character. The smaller the fluctuation amplitude, the more accurate and clear nucleation effects can be studied in free flow outside of bottlenecks. Model fluctuations in synchronized flow simulate driver time delay in deceleration, which is responsible for wide moving jam emergence in synchronized flow. To simulate this driver overdeceleration in synchronized flow, greater model fluctuations are applied.

A choice of δx determines the accuracy of vehicle speed calculations *in comparison* with the initial continuum in space stochastic model of [11,13]. We have found that the discrete model exhibits similar characteristics of phase transitions and resulting congested patterns at highway bottlenecks as those in the continuum model at δx that satisfies the conditions

$$\delta x/\tau^2 \ll b, a^{(\mathrm{a})}, a^{(\mathrm{b})}, a^{(0)}. \tag{B2}$$

[1] R. Herman, E. W. Montroll, R. B. Potts, and R. W. Rothery, Oper. Res. **7**, 86 (1959).

[2] D. C. Gazis, R. Herman, and R. W. Rothery, Oper. Res. **9**, 545 (1961).

[3] E. Kometani and T. Sasaki, J. Oper. Res. Soc. Jpn. **2**, 11 (1958); Oper. Res. **7**, 704 (1959).

[4] A. D. May, *Traffic Flow Fundamentals* (Prentice-Hall, Inc., New Jersey, 1990); M. Cremer, *Der Verkehrsfluss auf Schnellstrassen* (Springer, Berlin, 1979); W. Leutzbach, *Introduction to the Theory of Traffic Flow* (Springer, Berlin, 1988); *Traffic Flow Theory*, edited by N. H. Gartner, C. J. Messer, and A. Rathi (Transportation Research Board, Washington, D.C. 2001); D. C. Gazis, *Traffic Theory* (Springer, Berlin, 2002); D. Chowdhury, L. Santen, A. Schadschneider, Phys. Rep. **329**, 199 (2000); D. Helbing, Rev. Mod. Phys. **73**, 1067 (2001); T. Nagatani, Rep. Prog. Phys. **65**, 1331 (2002); K. Nagel, P. Wagner, and R. Woesler, Oper. Res. **51**, 681 (2003); R. Mahnke, J. Kaupužs, and I. Lubashevsky, Phys. Rep. **408**, 1 (2005); H. Rakha, P. Pasumarthy, and S. Adjerid, Transp. Lett. **1**, 95 (2009).

[5] B. S. Kerner and P. Konhäuser, Phys. Rev. E **50**, 54 (1994).

[6] B. S. Kerner, Phys. Rev. Lett. **81**, 3797 (1998).

[7] B. S. Kerner, *The Physics of Traffic* (Springer, Berlin, 2004).

[8] B. S. Kerner and S. L. Klenov, J. Phys. A **39**, 1775 (2006).

[9] B. S. Kerner, in *Encyclopedia of Complexity and System Science*, edited by R. A. Meyers (Springer, Berlin, 2009), pp. 9302–9355.

[10] B. S. Kerner, *Introduction to Modern Traffic Flow Theory and Control: The Long Road to Three-Phase Traffic Theory* (Springer, Berlin, 2009).

[11] B. S. Kerner and S. L. Klenov, J. Phys. A **35**, L31 (2002).

[12] B. S. Kerner, S. L. Klenov, and D. E. Wolf, J. Phys. A **35**, 9971 (2002).

[13] B. S. Kerner and S. L. Klenov, Phys. Rev. E **68**, 036130 (2003).

[14] L. C. Davis, Phys. Rev. E **69**, 016108 (2004).

[15] H. K. Lee, R. Barlović, M. Schreckenberg, and D. Kim, Phys. Rev. Lett. **92**, 238702 (2004).

[16] R. Jiang and Q.-S. Wu, J. Phys. A **37**, 8197 (2004).

[17] Kun Gao, Rui Jiang, Shou-Xin Hu, Bing-Hong Wang, and Qing-Song Wu, Phys. Rev. E **76**, 026105 (2007).

[18] J. A. Laval, in *Traffic and Granular Flow'05*, edited by A. Schadschneider, T. Pöschel, R. Kühne, M. Schreckenberg, and D. E. Wolf (Springer, Berlin, 2007), pp. 521–526.

[19] S. Hoogendoorn, H. van Lint, and V. L. Knoop, Transp. Res. Rec. **2088**, 102 (2008).

[20] L. C. Davis, Physica A **368**, 541 (2006); **361**, 606 (2006); **379**, 274 (2007); R. Jiang, M.-B. Hua, R. Wang, and Q.-S. Wu, Phys. Lett. A **365**, 6 (2007); R. Jiang and Q.-S. Wu, Phys. Rev. E **72**, 067103 (2005); Physica A **377**, 633 (2007); R. Wang, R. Jiang, Q.-S. Wu, and M. Liu, *ibid.* **378**, 475 (2007); A. Pottmeier, C. Thiemann, A. Schadschneider, and M. Schreckenberg, in *Traffic and Granular Flow'05*, edited by A. Schadschneider, T. Pöschel, R. Kühne, M. Schreckenberg, and D. E. Wolf (Springer, Berlin, 2007), pp. 503–508; X. G. Li, Z. Y. Gao, K. P. Li, and X. M, Zhao, Phys. Rev. E **76**, 016110 (2007); J. J. Wu, H. J. Sun, and Z. Y. Gao, *ibid.* **78**, 036103 (2008).

[21] We can expect that the physical theory of phase transitions occurring in vehicular traffic on multilane roads presented in the paper can be a basis for the further development of new traffic flow models and some interesting transportation applications. However, methodological aspects of traffic flow modeling and possible applications that can follow from the physical theory presented here are out of the scope of this paper and will be considered elsewhere.

[22] B. S. Kerner, Transp. Res. Rec. **1678**, 160 (1999); Phys. World **12**(8), 25 (1999).

[23] See formulas (16.31) and (16.32) of Ref. [7]: at $S_{n+1}=0$ speed fluctuations $\xi_n=0$.

[24] Because traffic flow at bottlenecks is usually nonhomogeneous and in the continuum model there are model fluctuations in nonhomogeneous traffic flow, the discrete model exhibits qualitatively the same simulation results of phase transitions at bottlenecks on multilane road as those derived with the continuum model.

[25] Therefore, this overacceleration model could be recommended for general use.

[26] Next Generation Simulation Programs (NGSIM), http://ngsim.camsys.com/

[27] S. Ahn and M. J. Cassidy, in *Transportation and Traffic Theory*, edited by R. E. Allsop, M. G. H. Bell, and B. G. Hydecker (Elsevier, Amsterdam, 2007), pp. 691–710.

[28] B. S. Kerner, Phys. Rev. E **65**, 046138 (2002).

[29] The latter has been proven in simulations made that show qualitatively the same physical effects as presented below, when only one on-ramp and one off-ramp on a road section are used.

[30] A more detailed data analysis and simulations of possible effects of a cascade of lane changing between three or more lanes is out of scope of this paper and will be published elsewhere.

[31] The qualitative difference between the MSP and wide moving jam is that an MSP is caught at a bottleneck, when the MSP reaches the bottleneck at which traffic breakdown is possible (the definition [S]) [7,28]. In contrast, the wide moving jam propagates through this bottleneck while maintaining the mean velocity of the downstream jam front (the definition [J]).

[32] B. S. Kerner, S. L. Klenov, and A. Hiller, J. Phys. A **39**, 2001 (2006); B. S. Kerner, S. L. Klenov, A. Hiller, and H. Rehborn, Phys. Rev. E **73**, 046107 (2006).

[33] Empirical data shown in Figs. 10(b) and 10(c) have been explained in [34,35] by a "boomerang effect," i.e., "growing perturbations on a homogeneous freeway section without on- and off-ramps" [34] leading to an F→J transition without bottlenecks (the origin of the axis for road locations was chosen differently in [34,35] and in Fig. 10: $x=0$ km in Fig. 10 is related to $x=465.1$ km of related figures of [34,35]). The empirical and numerical analyses presented in Sec. VI C show that the conclusion of [34,35] that the boomerang effect is the reason for wide moving jam emergence in Fig. 10 is *invalid*. In a more detail, criticisms of studies of traffic congestion made in [34,35] can be found in Sec. 10.3 of [10].

[34] M. Schönhof and D. Helbing, Transp. Sc. **41**, 135 (2007).

[35] M. Schönhof and D. Helbing, Transp. Res., Part B: Methodol. **43**, 784 (2009).

[36] Recall that the microscopic structure of a wide moving jam consists of a spatiotemporal combination of flow interruption

intervals that satisfy (15) and moving blanks, i.e., regions without vehicles moving upstream within the jam; the moving blanks are associated with vehicle motion at a very low speed within the jam [32].

[37] B. S. Kerner. J. Phys. A: Math. Theor. **41**, 215101 (2008); **41**, 369801 (2008).

[38] The averaging time interval T_{av} for the average flow rate $q^{(cong)}$ is assumed to be considerably longer than time distances between any moving jams within a congested pattern, for example, $T_{av} \gtrsim 30$ min.

[39] B. S. Kerner, in *Encyclopedia of Complexity and System Science*, edited by R. A. Meyers (Springer, Berlin, 2009), pp. 9355–9411.

[40] S. Krauss, P. Wagner, and C. Gawron, Phys. Rev. E **55**, 5597 (1997); S. Krauss, Ph.D. thesis, University of Cologne, 1998.

[41] P. G. Gipps, Transp. Res., Part B: Methodol. **15**, 105 (1981).